

# $\chi$ -colorable graph states: closed-form expressions and quantum orthogonal arrays

Konstantinos-Rafail Revis<sup>1,2,\*</sup> , Hrachya Zakaryan<sup>1,2</sup>   
and Zahra Raissi<sup>1,2</sup> 

<sup>1</sup> Department of Computer Science, Paderborn University, Warburger Str. 100, 33098 Paderborn, Germany

<sup>2</sup> Institute for Photonic Quantum Systems (PhoQS), Paderborn University, Warburger Str. 100, 33098 Paderborn, Germany

E-mail: [krevis@mail.uni-paderborn.de](mailto:krevis@mail.uni-paderborn.de), [hzak@mail.uni-paderborn.de](mailto:hzak@mail.uni-paderborn.de) and [zraissi@mail.uni-paderborn.de](mailto:zraissi@mail.uni-paderborn.de)

Received 1 April 2025; revised 23 July 2025

Accepted for publication 21 August 2025

Published 1 September 2025



CrossMark

## Abstract

Graph states are a fundamental class of multipartite entangled quantum states with wide-ranging applications in quantum information and computation. In this work, we develop a systematic approach for constructing and analyzing  $\chi$ -colorable graph states, deriving explicit closed-form expressions for arbitrary  $\chi$ . For a broad family of two- and three-colorable graph states, the representations obtained using only local operations require a minimal number of terms in the  $Z$ -eigenbasis. We prove that every two-colorable graph state is local Clifford (LC) equivalent to a state expressible as a summation of rows of an orthogonal array (OA). For graph states with  $\chi > 2$ , we show that they are LC-equivalent to quantum OAs, establishing a direct combinatorial connection between multipartite entanglement and structured quantum states. Furthermore, the upper and lower bounds of the Schmidt measure for graph states with arbitrary  $\chi$  colorability are discussed, extending the results for an arbitrary local dimension. Our results offer an efficient and practical method for systematically constructing graph states, optimizing their representation

\* Author to whom any correspondence should be addressed.



Original Content from this work may be used under the terms of the [Creative Commons Attribution 4.0 licence](https://creativecommons.org/licenses/by/4.0/). Any further distribution of this work must maintain attribution to the author(s) and the title of the work, journal citation and DOI.

in quantum circuits, and identifying structured forms of multipartite entanglement. This approach also connects graph states to  $k$ -uniform and absolutely maximally entangled states, motivating further exploration of the structure of entangled states and their applications in quantum networks, quantum error correction, and measurement based quantum computing.

Keywords: graph states, qudits, multipartite entanglement, quantum orthogonal arrays

## 1. Introduction

Multipartite entanglement is a fundamental resource in quantum information science [1], playing a central role in quantum computing, quantum error correction [2–5], quantum networks [6], and quantum cryptography [7]. Among the many families of entangled quantum states, graph states provide a structured way to encode entanglement, making them particularly useful for quantum error correction and measurement-based quantum computation [3, 8–12]. Given their connection to stabilizer codes [13], it is natural to explore whether the structural properties of graphs can reveal deeper insights into the computational power, entanglement properties, and classification of graph states.

One such structural property is the *chromatic number*, which describes the minimum number of colors required to assign to the vertices of a graph such that no two adjacent vertices share the same color [14]. The chromatic number is typically referred to as *colorability*. While colorability is a well-studied problem in classical graph theory, its role in the entanglement structure of graph states remains largely unexplored. Previous works have suggested that colorability places upper and lower bounds on the Schmidt measure of graph states [9] and that almost all two-colorable graph states have maximal Schmidt measure [15].

In this work, we develop a systematic approach for deriving closed-form expressions for two-colorable graph states. We begin by showing that such states are Locally-Clifford (LC)-equivalent to a summation over rows of a classical orthogonal array (OA) [16, 17]. In our work we show the direct connection between two-colorable graph states and the OAs. This result provides an efficient way to construct and manipulate highly entangled graph states, revealing a deep connection between the structure of graph states and combinatorial designs. Moreover, since OAs of index unity correspond to classical maximum distance separable codes [17], this implies a structural link between two-colorable graph states and optimal classical codes.

We then extend this approach to three-colorable graph states, proving that they are LC-equivalent to quantum OAs (QOAs) [17–21], and therefore can be useful in the context of their applications [22, 23]. This result highlights an intrinsic combinatorial structure in multipartite entangled states and provides an intuitive, efficient method for writing highly entangled three-colorable states directly from their graph structure. For the generic case, lower bounds on the Schmidt measure are obtained. Additionally, we analyze a special class of three-colorable graph states that include  $k$ -uniform and absolutely maximally entangled (AME) states [24], showing how additional graph connections modify entanglement properties.

To further explore the implications of colorability, we investigate the relationship between two- and three-colorable graph states under local unitary (LU) and LC operations. While LC operations can alter graph connectivity and consequently the colorability, because of local complementation [25–27], we discuss how we can determine the Schmidt measure of graph states with  $\chi > 2$ . Furthermore, we identify cases where three-colorable graph states cannot be transformed back into their corresponding two-colorable forms using any invertible local

operations [28], highlighting fundamental constraints imposed by graph connectivity on multipartite entanglement.

Finally, we extend our approach to arbitrary  $\chi$ -colorable graph states, providing closed-form expressions and examining their entanglement structure by obtaining bounds on Schmidt measure. Our approach demonstrates that higher-colorable graph states exhibit entanglement patterns that relate to QOAs, offering insights into multipartite entanglement characterization. While the computational complexity of colorability remains a challenge, our results suggest that it provides a structured way to analyze entangled states, with potential applications in quantum networks and scalable quantum computing architectures.

The remainder of this paper is organized as follows. In section 2, the basics of qudits and graph states are presented. In section 3, we derive a closed-form expression for two-colorable graph states and analyze its consequences for state construction and entanglement measures. In section 4, the closed-form expression and the corresponding impacts for the three-colorable graph states are displayed. Then, in section 5, we discuss a specialized set of three-colorable graph states designed to describe  $k$ -uniform states. In section 6, the usage of local complementation and the connection of the given approach to the  $k$ -uniform states is made apparent, indicating the impact of the previously presented results. In section 7, we generalize our results to arbitrary  $\chi$  colorability, further expanding the scope of our approach. Finally, we conclude in section 8 by discussing the potential implications of our work and outlining directions for future research.

## 2. Basics of qudit graph states

Graph states are highly entangled quantum states associated with a mathematical graph  $(V, E)$ , where vertices  $V$  represent qudits, and edges  $E$  correspond to entangling operations between them [29, 30]. These states serve as a central resource in quantum information protocols, including measurement-based quantum computation. Here, we introduce the essential formalism for qudit graph states, setting the stage for an exploration of their colorability in the following sections. Two vertices  $i, j \in V$ , with the total number of vertices denoted as  $n$ , are called adjacent if they are the endpoints of an edge.

The adjacency matrix  $\Gamma$  is a symmetric  $n \times n$  matrix defined over a finite field  $\mathbb{F}_d$ , where each nonzero element  $\Gamma_{ij} = \theta_{ij} \in \mathbb{F}_d$  specifies the entanglement weight between qudits  $i$  and  $j$  as noted in [31]:

$$\Gamma_{ij} = \begin{cases} \theta_{ij} & \text{if } i, j \in E \\ 0 & \text{otherwise} \end{cases}. \quad (1)$$

It must be underlined that we consider the finite field  $\mathbb{F}_d$ , where  $d$  is a prime number. Mentioning the neighborhood  $N_i \subset V$  of a graph  $G$  is useful, which is the set of vertices for which  $\{i, j\} \in E$ . Let us briefly review the concept of qudits, which are systems with  $d$  levels, such that the Hilbert space of each qudit is  $\mathbb{C}^d$ . The action of the Pauli operators  $Z$  and  $X$  on the eigenstates of  $Z$  is defined as follows [32, 33],

$$X^a|i\rangle = |i+a\rangle \quad \text{and} \quad Z^a|i\rangle = \omega^{ia}|i\rangle, \quad (2)$$

where  $\omega = e^{i2\pi/d}$  the  $d$ th root of unity,  $a \in \mathbb{F}_d$ , and  $X^d = Z^d = \mathbb{I}_d$ . All additions are performed modulo  $d$ . A critical operation for qudits is the Hadamard gate, whose action is defined as:

$$H|i\rangle = \frac{1}{\sqrt{d}} \sum_{l=0}^{d-1} \omega^{il}|l\rangle, \quad \text{and} \quad H^\dagger|i\rangle = \frac{1}{\sqrt{d}} \sum_{l=0}^{d-1} \omega^{-il}|l\rangle. \quad (3)$$

It must be noted that the Hadamard gate is more properly called the Fourier matrix, when referring to qudits, though we will use the former. Analogous to the qubit case, the controlled-Z (CZ) gate is defined for qudits as:

$$C_1 Z_2^\beta |i\rangle_1 |j\rangle_2 = \omega^{ij\beta} |i\rangle_1 |j\rangle_2, \quad (4)$$

where  $\beta \in \mathbb{F}_d$ . The subscripts in CZ indicate the control (first qudit) and target (second qudit), but since CZ is symmetric under the exchange of qudits, its effect remains unchanged if the indices are swapped. In contrast, for controlled-X (CX), the order of the indices is crucial: the first index corresponds to the control qudit, while the second index receives the modular addition transformation,

$$C_1 X_2^\gamma |i\rangle_1 |j\rangle_2 = |i\rangle_1 |i+j+\gamma\rangle_2, \quad (5)$$

where  $\gamma \in \mathbb{F}_d$ . In this case, the order of the indices is significant.

Finally, some useful relations relevant to the upcoming results are presented in appendix A. For a graph  $(V, E)$ , where  $V$  and  $E$  denote the sets of vertices ( $|V| = n$ ) a graph state is defined as [9]:

$$|\psi_{\text{GS}}\rangle = \left( \prod_{\{k,j\} \in E} C_k Z_j^{\Gamma_{kj}} \right) |+\rangle^{\otimes n},$$

where  $|+\rangle = H|0\rangle$  and  $|+\rangle^{\otimes n} = |+\rangle_1 \otimes \dots \otimes |+\rangle_n$ . (6)

For example, if we consider a qubit, with  $n = 3$  and the graph is a triangle, utilizing the above definition, we have:

$$|\psi_{\text{GS}}\rangle = \frac{1}{2\sqrt{2}} (|000\rangle + |001\rangle + |010\rangle + |100\rangle - |011\rangle - |101\rangle - |110\rangle + |111\rangle). \quad (7)$$

It should be noted that the normalization factor here is not omitted but, in general, is omitted unless it is essential to the discussion. Here, the subscript GS indicates that the state  $|\psi_{\text{GS}}\rangle$  corresponds to the graph representation.

### 3. Two-colorable graph states

Let  $|\psi_{2\text{-color}}\rangle$  be a two-colorable graph state. A graph is two-colorable if its chromatic number is  $\chi = 2$ , meaning that its vertices can be partitioned into two disjoint sets, which we label as  $B$  (blue vertices) and  $R$  (red vertices). The total number of red vertices is  $n_R$ , and the total number of blue vertices is  $n_B$ , so the total number of vertices in the graph is  $n = n_R + n_B$ . Throughout this section, the notation  $r \in R$  refers to a qudit in the set of red vertices, and  $b \in B$  refers to a qudit in the set of blue vertices.

We assume that the CZ operations in the graph state construction occur between red vertices as controls and blue vertices as targets. The two-colorable graph state  $|\psi_{2\text{-color}}\rangle$ , is then expressed as:

$$|\psi_{2\text{-color}}\rangle = \prod_{r \in R, b \in B} C_r Z_b^{\Gamma_{rb}} |+\rangle^{\otimes R} |+\rangle^{\otimes B}, \quad (8)$$

where the notation  $|+\rangle^{\otimes R}$  denotes that every red qudit is prepared in  $|+\rangle$  state and similarly for  $|+\rangle^{\otimes B}$ . This expression highlights the structural simplicity of two-colorable graph states,

as the adjacency matrix of any two-colorable graph state takes a specific block form

$$\Gamma_{2\text{-color}} = \Gamma_{rb} = \left( \begin{array}{c|c} \overbrace{O}^B & \overbrace{A_{RB}}^R \\ \hline \overbrace{A_{RB}^T} & \overbrace{O} \end{array} \right), \quad (9)$$

where the block  $A_{RB}$  is the  $n_R \times n_B$  block containing the weights of edges connecting red and blue vertices. The diagonal blocks are zero matrices because vertices of the same color are not connected in two-colorable graphs.

Two-colorable graph states have significant applications in quantum error correction, measurement-based quantum computing, and entanglement quantification [34, 35]. In the following, we derive a closed-form representation for two-colorable graph states and explore their implications for their construction, analysis, and applications. Before proceeding it has to be mentioned that from now and on when it is written  $\sum_{\vec{k}=0}^{d-1}$  and  $\vec{k} = (k_1, \dots, k_n)$  is a row vector with  $n$  elements it is a short hand notation for  $\sum_{k_1=0}^{d-1} \dots \sum_{k_n=0}^{d-1}$ .

**Proposition 1.** *Let  $|\psi_{2\text{-color}}\rangle$  be a two-colorable graph state characterized by an adjacency matrix  $\Gamma_{2\text{-color}}$ . Let  $n_B$  and  $n_R$  denote the number of blue and red vertices, respectively. Assuming without loss of generality  $n_B \geq n_R$ , every two-colorable state satisfies the following closed-form expression:*

$$H^{\dagger \otimes B} |\psi_{2\text{-color}}\rangle = \sum_{\vec{i}=0}^{d-1} |\vec{i}\mathcal{G}\rangle, \quad (10)$$

where  $\vec{i} = (i_1, i_2, \dots, i_{n_R})$  is a row vector of  $n_R$  elements, and  $\mathcal{G} = [\mathbb{I}_{n_R} \mid A_{RB}]$ , with  $A_{RB}$  being the top-right block of the adjacency matrix  $\Gamma_{2\text{-color}}$ .

**Proof.** To prove the closed-form expression for  $|\psi_{2\text{-color}}\rangle$ , we assume without loss of generality that  $n_B \geq n_R$ . By applying  $H^\dagger$  to every blue qudit, we start with:

$$H^{\dagger \otimes B} |\psi_{2\text{-color}}\rangle = \prod_{r \in R, b \in B} H^{\dagger \otimes B} C_r Z_b^{\Gamma_{rb}} |+\rangle^{\otimes R} |+\rangle^{\otimes B}.$$

Using the commutation relation  $H^\dagger ZH = X$  for Pauli operators, the  $H^\dagger$  gate commutes with the CZ operation as, (see also (A.1)),

$$H^\dagger C_r Z_b^{\Gamma_{rb}} = C_r X_b^{\Gamma_{rb}} H^\dagger.$$

Substituting this commutation relation, we obtain:

$$H^{\dagger \otimes B} |\psi_{2\text{-color}}\rangle = \prod_{r \in R, b \in B} C_r X_b^{\Gamma_{rb}} |+\rangle^{\otimes R} H^{\dagger \otimes B} H^{\otimes B} |0\rangle^{\otimes B},$$

and thus:

$$H^{\dagger \otimes B} |\psi_{2\text{-color}}\rangle = \prod_{r \in R, b \in B} C_r X_b^{\Gamma_{rb}} |+\rangle^{\otimes R} |0\rangle^{\otimes B}.$$

Recalling that  $|+\rangle = H|0\rangle$ , the state becomes:

$$H^{\dagger \otimes B} |\psi_{2\text{-color}}\rangle = \sum_{\vec{i}=0}^{d-1} \prod_{r \in R, b \in B} C_r X_b^{\Gamma_{rb}} |i_1 \dots i_{n_R}\rangle |0\rangle^{\otimes B}.$$

Applying the CX operation, the blue qudits are updated as:

$$H^{\dagger \otimes B} |\psi_{2\text{-color}}\rangle = \sum_{\vec{i}=0}^{d-1} \prod_{r \in R, b \in B} |i_1 \dots i_{n_R}\rangle X_b^{\Gamma_{rb} \cdot i_r} |0\rangle^{\otimes B}.$$

For each blue qudit  $b \in B$ , the  $X_b$  operator applies shifts determined by the sum of neighboring red qudit indices:

$$H^{\dagger \otimes B} |\psi_{2\text{-color}}\rangle = \sum_{\vec{i}=0}^{d-1} \prod_{b \in B} |i_1 \dots i_{n_R}\rangle X_b^{\sum_{r \in R} \Gamma_{rb} \cdot i_r} |0\rangle^{\otimes B}.$$

Finally, applying the  $X_b$  operators to  $|0\rangle^{\otimes B}$  yields:

$$H^{\dagger \otimes B} |\psi_{2\text{-color}}\rangle = \sum_{\vec{i}=0}^{d-1} |i_1 \dots i_{n_R}\rangle \bigotimes_{b \in B} \left| \sum_{r \in R} \Gamma_{rb} \cdot i_r \right\rangle.$$

The indices of the red qudits form a row vector  $\vec{i} = (i_1, i_2, \dots, i_{n_R})$  and defining the generator matrix as  $\mathcal{G} = \begin{bmatrix} \mathbb{I}_{n_R} & A_{RB} \end{bmatrix}$ , where  $A_{RB}$  is the top right block of adjacency matrix  $\Gamma_{2\text{-color}}$ , the equation simplifies to:

$$H^{\dagger \otimes B} |\psi_{2\text{-color}}\rangle = \sum_{\vec{i}=0}^{d-1} |\vec{i}\mathcal{G}\rangle. \tag{11}$$

This concludes the proof of the closed-form expression. □

This result of the proposition 1 provides a direct, step-by-step method for constructing the state vector of any two-colorable graph state. The procedure is as follows:

- Step 1: In a two-colorable graph, identify the red and blue vertex sets ( $R$  and  $B$ ). Without loss of generality, we have assumed  $n_B \geq n_R$ .
- Step 2: Assign indices to the red vertices.
- Step 3: Compute the indices for the blue vertices as the sum of their neighboring red vertex indices.
- Step 4: Combine these assignments into the state expression and sum over the red vertex indices.

To demonstrate the utility of proposition 1, let us consider two examples: a six-qudit circular graph and a six-qudit cluster graph figure 1.

**Example 1.** Six-qudit circular graph: Using the graph in figure 1(a), the graph state is written using the definition in equation (8) as:

$$|\Psi_{GS}\rangle = \sum_{i_1, \dots, i_6=0}^{d-1} \omega^{i_1 i_4} \omega^{i_4 i_2} \omega^{i_2 i_5} \omega^{i_5 i_3} \omega^{i_3 i_6} \omega^{i_6 i_1} |i_1, i_2, i_3\rangle |i_4, i_5, i_6\rangle. \tag{12}$$

In this example, the red vertices are labeled as  $\{i_1, i_2, i_3\}$ , and the blue vertices are  $\{i_4, i_5, i_6\}$ . Using proposition 1, we assign indices  $i_1, i_2, i_3$  to the red vertices. For the blue vertices, their indices are determined as the summation of the indices of their neighboring red vertices. For instance:

$$i_4 = i_1 + i_2, \quad i_5 = i_2 + i_3, \quad \text{and} \quad i_6 = i_3 + i_1. \tag{13}$$

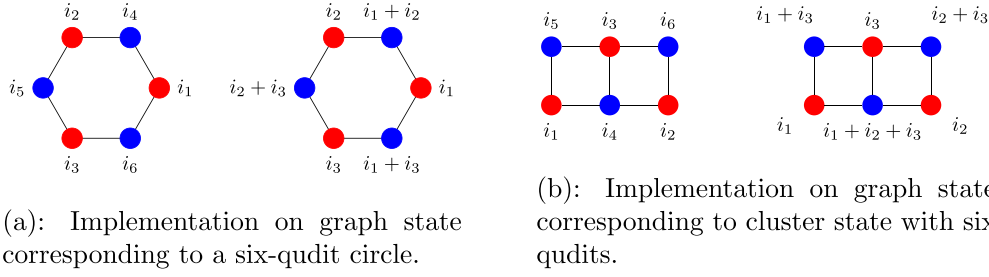


**Figure 1.** Two examples of the implementation of the formula obtained in the proposition 1. On the left of each sub-figure, we have the indices assigned using the definition of graph states given by equation (8), and on the right, we have the assignment of indices using the obtained result.

The closed-form expression directly follows:

$$|\psi_{\text{closed-form}}\rangle = \sum_{i_1, i_2, i_3=0}^{d-1} |i_1, i_2, i_3\rangle |i_1 + i_2, i_2 + i_3, i_3 + i_1\rangle. \quad (14)$$

This example demonstrates how to use the graph's structure to implement the closed-form expression.

**Example 2.** Six-qudit cluster graph: For the graph in figure 1(b), the graph state is expressed using equation (8) as:

$$|\Psi_{\text{GS}}\rangle = \sum_{i_1, \dots, i_6=0}^{d-1} \omega^{i_1 i_5} \omega^{i_1 i_4} \omega^{i_3 i_5} \omega^{i_3 i_4} \omega^{i_3 i_6} \omega^{i_2 i_4} \omega^{i_2 i_6} |i_1, i_2, i_3\rangle |i_4, i_5, i_6\rangle. \quad (15)$$

Here, again the red vertices are  $\{i_1, i_2, i_3\}$ , and the blue vertices are  $\{i_4, i_5, i_6\}$ . Assigning indices  $i_1, i_2, i_3$  to the red vertices, the indices of the blue vertices are computed as:

$$i_4 = i_1 + i_2 + i_3, \quad i_5 = i_1 + i_3, \quad \text{and} \quad i_6 = i_2 + i_3. \quad (16)$$

The closed-form expression is:

$$|\psi_{\text{closed-form}}\rangle = \sum_{i_1, i_2, i_3=0}^{d-1} |i_1, i_2, i_3\rangle |i_1 + i_2 + i_3, i_1 + i_3, i_2 + i_3\rangle. \quad (17)$$

Proposition 1 has important implications for the Schmidt measure of two-colorable graph states. From [9], any state vector  $|\phi\rangle \in \mathcal{H}^{(1)} \otimes \dots \otimes \mathcal{H}^{(n)}$  of a compound quantum system with  $n$  components can be expressed as:

$$|\phi\rangle = \sum_{i=1}^{\Lambda} \zeta_i |\phi_i^{(1)}\rangle \otimes \dots \otimes |\phi_i^{(n)}\rangle, \quad (18)$$

where  $\zeta_i \in \mathbb{C}$  for  $i = 1, \dots, \Lambda$  and  $|\phi_i^{(j)}\rangle \in \mathcal{H}^{(j)}$ . Bearing this information into account, the Schmidt measure is defined as [9, 36]:

$$E_s(|\psi\rangle) = \log_2(\lambda), \quad (19)$$

where  $\lambda$  is the minimal number  $\Lambda$  of the terms in the sum presented in (18), over every linear decomposition into product states. Proposition 7 of [9] provides upper and lower bounds for the Schmidt measure of a qubit two-colorable graph state.

$$\frac{1}{2} \text{rank}(\Gamma_{2\text{-color}}) \leq E_s(|\psi_{2\text{-color}}\rangle) \leq \lfloor \frac{n_B + n_R}{2} \rfloor. \tag{20}$$

This result extends to any local dimension. The proof for the lower bound is given in appendix B, while the upper bound can be straightforwardly generalized as is done in [9]. This means that if  $\Gamma_{2\text{-color}}$  is a full rank matrix, the upper and lower bounds of equation (20) are the same. So in this case, the closed form expression given in proposition 1 provides the minimum number of terms in the  $Z$ -eigenbasis. For instance, every cluster state, like the one given in figure 1(b), fulfills these requirements.

According to our result given in proposition 1, when  $H^\dagger$  is applied to every blue qudit, the number of terms obtained in the closed-form is  $d^{n_R}$ . This outcome has important implications for computational purposes. The reason is that following the standard definition of a graph state  $|\psi_{\text{GS}}\rangle$  given in equation (6), one has to explicitly evaluate the full state vector in the computational basis by summing over  $d^{n_R+n_B}$  terms each of which are weighted by a product of phase factors up to  $\mathcal{O}((n_R + n_B)^2)$  stemming from the graph structure and the adjacency matrix  $\Gamma_{2\text{-color}}$  given in equation (9). In contrast, our closed-form expression for graph states allows us to compute the full state by summing over only  $d^{n_R}$  terms while the phase factors are completely eliminated. For each term of the vector  $i\vec{\mathcal{G}}$ , one has to multiply a row vector with length  $n_R$  with the  $n_R \times (n_R + n_B)$  generator matrix  $\vec{\mathcal{G}}$ . Therefore, it is apparent that with our closed-form expression the exponential scaling is reduced from  $d^n$  to  $d^{n_R}$ , which can be significantly smaller when  $n_R \ll n_B$ .

A final important implication of proposition 1 is that every two-colorable graph state can be written as a state that can be defined based on an OA. According to [16], an OA denoted as  $OA(r, n, d, k)$  is a positioning formed up by  $r$  rows,  $n$  columns, and the entries are taking values ranging from the set  $\{0, \dots, d - 1\}$ . An important property is that every subset with  $k$  columns has all the combinations of symbols, which occur the same number of times through the rows. To clarify this idea, let us discuss an example. The  $OA(4, 4, 2, 2)$  that has 4 rows, 4 columns, 2 levels per factor, and a strength of 2. This means that for any two columns chosen, all combinations of the levels 0 and 1 will appear equally across the trials. As an example, the following can be written:

$$\begin{matrix} 0 & 0 & 0 & 0 \\ 0 & 1 & 1 & 1 \\ 1 & 0 & 1 & 1 \\ 1 & 1 & 0 & 0 \end{matrix}.$$

Two OAs are equivalent if one can be transformed into the other by applying permutations or relabeling symbols within rows or columns.

As per [16], an OA can be defined if a row vector  $\vec{x} = (x_1, \dots, x_d)$  and a generator matrix of the form  $\mathcal{G} = [\mathbb{I}_d \mid M]$  are assumed where the matrix  $M$  is a  $d \times p$  matrix. Then, the OA can be written in the form  $OA = \vec{x} \cdot \mathcal{G}$ . The closed-form expression in proposition 1 takes precisely the OA form  $\vec{x} \cdot \mathcal{G}$ , establishing that every two-colorable graph state is LC-equivalent to a summation over rows of a classical OA. To our knowledge, this is the first result demonstrating this connection. As discussed in [19], OA-based states possess strong multipartite entanglement and are useful in quantum information protocols. Our result shows that these properties are universally present across all two-colorable graph states.

#### 4. Three-colorable graph states

Extending our analysis to three-colorable graph states ( $\chi = 3$ ), we now consider graphs where the vertex set can be partitioned into three disjoint subsets. Unlike the two-colorable case, three-colorability introduces additional structural complexity, and determining a valid 3-coloring is known to be NP-hard [37–39]. Let  $R, G, B$  denote the sets of blue, green, and red vertices, respectively, with cardinalities  $n_R, n_G$ , and  $n_B$ . The total number of vertices in the graph is then given by  $n = n_R + n_G + n_B$ . In our notation, choosing a vertex  $r \in R$  corresponds to selecting a red vertex, and similarly for  $b \in B$  and  $g \in G$ . Therefore  $|\psi_{3\text{-color}}\rangle$  is given as follows:

$$|\psi_{3\text{-color}}\rangle = \left( \prod_{r \in R, b \in B} C_r Z_b^{\Gamma_{rb}} \right) \left( \prod_{r \in R, g \in G} C_r Z_g^{\Gamma_{rg}} \right) \left( \prod_{g \in G, b \in B} C_g Z_b^{\Gamma_{gb}} \right) |+\rangle^{\otimes R \cup G \cup B}. \quad (21)$$

Partitioning the adjacency matrix into blocks clarifies the interactions between different color groups, allowing us to systematically construct the graph state. The adjacency matrix for  $\chi = 3$  is denoted as:

$$\Gamma_{3\text{-color-general}} = \begin{pmatrix} \overbrace{0}^R & \overbrace{A_{GR}}^G & \overbrace{A_{BR}}^B \\ \hline A_{GR}^T & 0 & A_{BG} \\ \hline A_{BR}^T & A_{BG}^T & 0 \end{pmatrix}. \quad (22)$$

Additionally, the matrix  $\mathcal{G}_{RB,GB}$  (additional connection between green and blue vertices compared to  $\mathcal{G}_{RB}$ ) is a generator-like matrix with dimensions  $(n_R + n_G) \times (n_R + n_G + n_B)$  defined as:

$$\mathcal{G}_{RB,GB} = \left[ \mathbb{I}_{n_R+n_G} \mid \begin{bmatrix} A_{BR} \\ A_{BG} \end{bmatrix} \right], \quad (23)$$

with  $A_{BR}$  and  $A_{BG}$  the corresponding blocks of matrix (22). For the upcoming discussion, it will also be helpful to note that the index  $g_j$  denotes a qudit having the green color and therefore  $j \in \{1, \dots, n_G\}$ . The vector  $(\vec{A}_{GR})_{g_j}$  denotes the vector constructed from extracting the row  $g_j$  of the matrix  $A_{GR}$ , which corresponds to the row containing all the elements of the adjacency matrix (22) that describe a specific green qudit  $g_j$ .

**Proposition 2.** *Let  $|\psi_{3\text{-color}}\rangle$  be a three-colorable graph state characterized by an adjacency matrix  $\Gamma_{3\text{-color-general}}$ . Let  $n_B, n_R$ , and  $n_G$  denote the number of blue, red and green vertices, respectively. Assuming without loss of generality  $n_B \geq n_G \geq n_R$ , every three-colorable state satisfies the following closed-form expression:*

$$H^{\dagger \otimes B} |\psi_{3\text{-color}}\rangle = \sum_{\vec{w}=0}^{d-1} \left( \bigotimes_{j=1}^{n_G} Z_{g_j}^{\vec{w} \cdot (\vec{A}_{GR})_{g_j}} \right) |\vec{w} \cdot \mathcal{G}_{RB,GB}\rangle, \quad (24)$$

where  $\vec{u} = (u_1, u_2, \dots, u_{n_R})$ ,  $\vec{v} = (v_1, \dots, v_{n_G})$  both row vectors, with  $n_R$  and  $n_G$  elements respectively, and  $\vec{w} = (\vec{u}, \vec{v})$  is the concatenation of  $\vec{u}$  and  $\vec{v}$ .

**Proof.** Let us start with the definition given in equation (21). Recalling equation (27), we can define the following row vectors  $\vec{u} = (u_1, u_2, \dots, u_{n_R})$ ,  $\vec{v} = (v_1, \dots, v_{n_G})$ . It is useful to define the

vector  $\vec{w} = (\vec{u}, \vec{v})$ , the concatenation of  $\vec{u}$  and  $\vec{v}$ . Let us perform the CZ operations that involve the blue qudits:

$$H^{\dagger \otimes B} |\psi_{3\text{-color}}\rangle = H^{\dagger \otimes B} \sum_{\vec{u}, \vec{v}=0}^{d-1} \prod_{r \in R, g \in G} C_r Z_g^{\Gamma_{rg}} |\vec{u}\rangle |\vec{v}\rangle \bigotimes_{b \in B} Z_b^{f_r(b)+f_g(b)} |+\rangle_b. \quad (25)$$

where  $f_r(b) = \sum_{r \in R} u_r \Gamma_{rb}$  and  $f_g(b) = \sum_{g \in G} v_g \Gamma_{gb}$ . We should note that, till this point, we have not performed the  $H^{\dagger \otimes B}$  operation. It is clear that since it is a local operation acting only on the blue qudits, it will commute via the remaining CZ operation between the green and the red qudits. This will lead to:

$$H^{\dagger \otimes b} Z_b^{f_r(b)+f_g(b)} = X_b^{f_r(b)+f_g(b)} H^{\dagger \otimes b}, \quad \text{with } b \in B. \quad (26)$$

This implies that:

$$H^{\dagger \otimes B} |\psi_{3\text{-color}}\rangle = \sum_{\vec{u}, \vec{v}=0}^{d-1} \left( \prod_{r \in R, g \in G} C_r Z_g^{\Gamma_{rg}} \right) |\vec{u}\rangle |\vec{v}\rangle \bigotimes_{b \in B} |f_r(b) + f_g(b)\rangle_b. \quad (27)$$

At this point, there is a remaining CZ operation between the green and the red qudits. Unfortunately, the trick of using another Hadamard gate can not be applied here. We have to understand that the primary goal is to find a way to obtain as few terms as possible in the Z-eigenbasis. In any case, we seek to reduce the number of phases in front of each bracket, but this would unavoidably increase the number of terms used in the Z-eigenbasis. We can define the matrix  $\mathcal{G}_{RB,GB}$ , which is generator-like matrix with dimensions  $(n_R + n_G) \times (n_R + n_G + n_B)$ , as:

$$\mathcal{G}_{RB,GB} = \left[ \mathbb{I}_{n_R+n_G} \mid \begin{bmatrix} A_{BR} \\ A_{BG} \end{bmatrix} \right], \quad (28)$$

with  $A_{BR}$  and  $A_{BG}$  the corresponding blocks of matrix (22). In this juncture, the equation (27) will read as:

$$H^{\dagger \otimes B} |\psi_{3\text{-color}}\rangle = \sum_{\vec{w}=0}^{d-1} \left( \prod_{r \in R, g \in G} C_r Z_g^{\Gamma_{rg}} \right) |\vec{w} \cdot \mathcal{G}_{RB,GB}\rangle, \quad (29)$$

where  $\vec{w} = 0$  denotes the range of the indices  $u_1, \dots, u_{n_R}, v_1, \dots, v_{n_G} = 0$ .

The final step is to realize the power of the adjacency matrix (22). Assume that the index  $g_j$  denotes a qudit having the green color and therefore  $j \in \{1, \dots, n_G\}$ . Finally, define the vector  $(\vec{A}_{GR})_{g_j}$ , to denote the vector constructed from extracting the row  $g_j$  of the matrix  $A_{GR}$ , which corresponds to the row containing all the elements of the adjacency matrix (22) that describe a specific green qudit  $g_j$ ,

$$H^{\dagger \otimes B} |\psi_{3\text{-color}}\rangle = \sum_{\vec{w}=0}^{d-1} \left( \bigotimes_{j=1}^{n_G} Z_{g_j}^{\vec{u} \cdot (\vec{A}_{GR})_{g_j}} \right) |\vec{w} \cdot \mathcal{G}_{RB,GB}\rangle.$$

This concludes our proof. □

At this point, we turn our focus to discussing the implications of proposition 2. Let us start with the fact that we are equipped with an easy way to write a general three-colorable graph state. Here, a step-by-step process is presented:

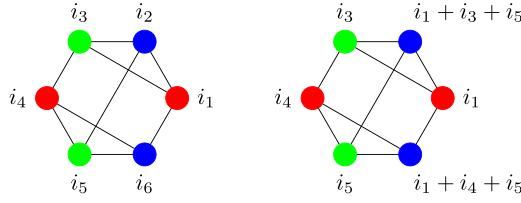


**Figure 2.** An example of implementation of the closed-form expression for a 6 qudit three-colorable graph state.

- Step 1: In a three-colorable graph identify the colors of the graph and assign the colors following that without loss of generality  $n_R \leq n_G \leq n_B$ .
- Step 2: Assign indices to the red and green qudits.
- Step 3: The indices of the blue qudits are the summation of the neighboring indices of each blue qudit weighted with the corresponding weight of the adjacency matrix.
- Step 4: To identify the correct exponent for the  $Z$  operations for each green qudit, we need to identify the red neighbors of each green qudit and multiply their indices scaled with the adequate weight imposed by the adjacency matrix (22)

The state given on the left-hand side of figure 2 can be written as:

$$|\psi_{GS}\rangle = \sum_{i_1, \dots, i_6=0}^{d-1} \omega^{i_1 i_2 + i_2 i_3 + i_3 i_4 + i_4 i_5 + i_5 i_6 + i_6 i_1 + i_1 i_3 + i_4 i_6 + i_2 i_5} |i_1, i_2, i_3, i_4, i_5, i_6\rangle. \quad (30)$$

Applying our methodology, the indices for the red and green qudits are kept as they were before, but the indices for the red qudits are given with respect to the red and green qudits, as the right-hand side of figure 2 indicates. With these steps, we have implemented steps 1 to 3. The determination of the correct exponents for the  $Z$  operators is easy, since one has to simply identify the green qudits that have a red connection. Then multiply the indices with the corresponding weight coming from the adjacency matrix, which in this case is one. So, the closed-form expression of this example is:

$$|\psi_{3\text{-color}}\rangle = \sum_{i_1, i_3, i_4, i_5=0}^{d-1} Z_{g_{i_3}}^{i_1 i_3 + i_3 i_4} Z_{g_{i_5}}^{i_4 i_5} |i_1, i_1 + i_3 + i_5, i_3, i_4, i_5, i_1 + i_4 + i_5\rangle. \quad (31)$$

To avoid confusion, the indices  $g_{i_3}$  and  $g_{i_5}$  are used to denote the  $Z$  operations acting on the green qudits that in figure 2, are denoted with indices  $i_3$  and  $i_5$ . It is important to note that there is a difference between the indexing to implement the closed-form expression and the indices to name and group the qudits according to their color. At this juncture, it has to be pointed out that the above example was not chosen randomly. According to [19], this state is also an AME state of six qudits with local dimension  $d$  being a prime number. We denote these states as  $\text{AME}(6, d)$ . In section 5 we are going to tailor the formalism presented here to better represent graph states that are highly entangled.

Our analysis shows that every three-colorable graph state can be rewritten in the form of a QOA, reinforcing the deep connection between graph states and highly entangled quantum states [17–20]. QOAs are combinatorial designs that contain rows composed of pure multipartite quantum states and exhibit high entanglement properties. Bearing in mind the definition of the classical OAs, the QOAs are constructed assuming specific parameters for the OA [40]. As previously mentioned, QOAs display high entanglement properties and therefore they can

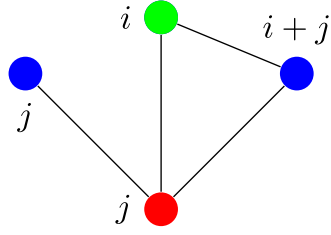


**Figure 3.** A simple example where our closed-form expression given in proposition 2 achieves the lower bound for the Schmidt measure.

be used to generate  $k$ -uniform states and AME states [18]. Additionally, they are rather useful in decoupling schemes in quantum networks [22, 23]. Various QOA setups have been studied in works like [19, 21].

In general, proposition 2 implies that every three-colorable graph state can be written as a QOA. Initially, it is trivial to understand that if the correct vector  $\vec{w}$  and the correct  $\mathcal{G}_{RB,GB}$  matrix, following the notation from proposition 2, is used then, the object  $\vec{w} \cdot \mathcal{G}_{RB,GB}$  represents an OA. The reason why any three-colorable graph, is in general, a QOA relies on the additional  $Z$  phases that we were not able to eliminate. In the scope of graph states, it is easy to understand if we recall that every three-colorable graph can become two-colorable if the appropriate number of edges is deleted. Reversing the process, adding edges to a two-colorable graph means that in general, we act with a non-local  $CZ$  operation between vertices that have the same color, and thus we create a three-colorable graph. This means that we are acting with a non-local operator on a state that is initially described by an OA. This implies that every three-colorable graph is described as a QOA since the so-called ‘quantumness of the QOA’ is modified as is mentioned in [19]. We refer the reader to the aforementioned work for a detailed analysis of this concept.

Another remark regarding proposition 2 is about the Schmidt measure of any three-colorable graph. As it is already explained in section 3, this discussion is essentially the same as finding the minimal number of terms required to describe the state in the  $Z$ -eigenbasis. The proof for the lower bound provided in appendix B can also be used here. Therefore, two bipartitions  $A$  and  $B$  are considered. In our formalism, the matrix  $\Gamma_{A|B}$  denotes the connections between the vertices of the sets  $A$  and  $B$ . In the case of  $\chi \geq 2$ , both bipartitions  $A$  and  $B$  can include more than one set of colors. Recalling the result of appendix B we arrive at:

$$\max \{ \text{rank}(\Gamma_{R|GB}), \text{rank}(\Gamma_{G|RB}), \text{rank}(\Gamma_{B|RG}) \} \leq E_s(|\psi_{3\text{-color}}\rangle). \quad (32)$$

For the upper bound, we refer to the discussion after proposition 7 in [9]. Any graph, which is not two-colorable, can be transformed into a two-colorable one by deleting the appropriate vertices on cycles with odd length. This corresponds to  $Z$  measurements. This idea can be straightforwardly generalized to qudits. Therefore, we can adapt the equation (20) as follows:

$$E_s(|\psi_{3\text{-color}}\rangle) \leq \lfloor \frac{n+K}{2} \rfloor, \quad (33)$$

where  $K$  is the number of vertices deleted. Figure 3 presents an example where the closed-form expression from proposition 2 yields the minimal number of terms in the  $Z$ -eigenbasis.

Before concluding this section, let us provide a formal discussion of the advantages of the closed-form expression from the computational aspect. Following the definition of a graph state given in equation (6),  $d^{n_R+n_G+n_B}$  terms need to be summed and each one of them needs

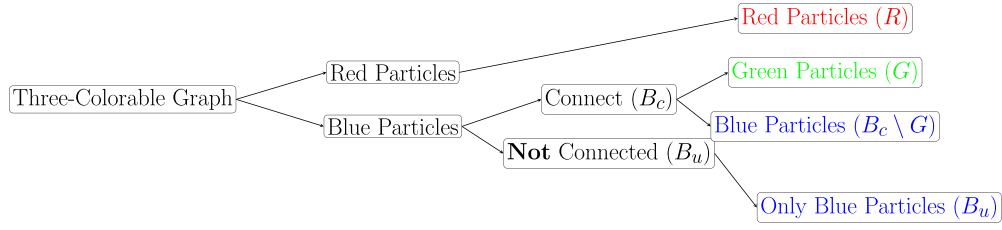


**Figure 4.** A schematic description of the creation of the three colorable graph states studied in this work.

to be weighted with a product of phases up to  $\mathcal{O}((n_R + n_G + n_B)^2)$ . For our result, we have a systematic way to reduce the number of summations to  $d^{n_R + n_G}$  and the number of required phases to  $\mathcal{O}((n_R + n_G)^2)$ . This improvement is important for computational purposes, especially when one wants to store this information or use the state for a classical simulation.

### 5. A special class of three-colorable graph states

We extend our analysis of three-colorable graph states to a special class tailored for the construction of  $k$ -uniform and AME states. This approach serves two main purposes. Firstly, these states are of particular interest in quantum information applications. Secondly, the presented methodology is an alternative approach to obtaining the closed-form expression for this special class of three-colorable graph states.

- Start with a two-colorable graph as the one assumed in section 3 for the graph state  $|\psi_{2\text{-color}}\rangle$ , therefore, in this case, the  $n_R \leq n_B$  without loss of generality once again.
- Assume that the blue qudits are separated into 2 disjoint sets named  $B_c$  and  $B_u$ . The number of blue qudits in the set  $B_c$  is  $n_{B_c}$  and the number of blue qudits in the set  $B_u$  is  $n_{B_u}$ .
- It is crucial to assume that  $n_R \leq n_{B_u}$ . In principle, we can also impose conditions on the relationship between  $n_R$  and  $n_{B_c}$ , but, as we are going to establish later on, this is not important. Therefore, without loss of generality, we are going to assume that  $n_R \leq n_{B_c}$ .
- Among the qudits belonging in the set  $B_c$ , without omitting any of the connections established in the initial graph, create a new two-colorable graph. This means that now the set of qudits, belonging to  $B_c$ , either remain blue qudits or change to become green qudits. The set of these green qudits is denoted as  $G$  and the total number of green qudits is denoted as  $n_G$ . The set of these blue qudits is denoted as  $B_c \setminus G$  and the total number of these blue qudits is denoted as  $n_{B_c \setminus G}$ . We impose without loss of generality that  $n_G \leq n_{B_c \setminus G}$ .
- The blue qudits belonging to  $B_u$  remain unaffected as they were in the 2-colorable graph state  $|\psi_{2\text{-color}}\rangle$ .

The above procedure is summarized in figure 4. Although it may look like many restrictions have appeared in the construction of this type of three colorable states, these setups have appeared in various contexts, for example for  $k$ -uniform states [28] or for cluster states, where a few qudits of the same color have been connected like in [41]. Bearing in mind this information,  $|\psi_{3\text{-color}}\rangle$  is defined as follows:

$$|\psi_{3\text{-color}}\rangle = \left( \prod_{b,b' \in B_c} C_b Z_{b'}^\Gamma \right) \left( \prod_{b \in B_c, r \in R} C_b Z_r^\Gamma \right) \left( \prod_{b \in B_u, r \in R} C_b Z_r^\Gamma \right) |+\rangle^{\otimes R \cup B_u \cup B_c}. \quad (34)$$

At this point, understanding the form of the adjacency matrix is crucial to proceed with our main results. Its form is given by equation (35):

$$\Gamma_{3\text{-color}} = \begin{pmatrix} \overbrace{\mathbf{0}}^R & \overbrace{\mathbf{A}_{B_u R}}^{B_u} & \overbrace{A_{B_c \setminus G}}^{B_c \setminus G} & \overbrace{A_{GR}}^G \\ \mathbf{A}_{B_u R}^T & \mathbf{0} & 0 & 0 \\ A_{B_c \setminus G}^T & 0 & \mathbf{0} & \mathbf{A}_{GB_c \setminus G} \\ A_{GR}^T & 0 & \mathbf{A}_{GB_c \setminus G}^T & \mathbf{0} \end{pmatrix}. \quad (35)$$

The comparison of the matrix (35) with the general form of the adjacency matrix of any three-colorable graph given in equation (22) is unavoidable. In both cases, the matrices given in equations (35) and (22) are block matrices. The non-zero blocks denoted with  $A$  and a subscript with two or more letters indicating the sets of different colored qudits, are assumed they be connected. It is also obvious that the matrix (22) is a generalization of the matrix (35). Finally, the reason we denoted with bold letters the part of the matrix (35) is to make apparent the condition we have imposed, firstly, one has to assume a two-colorable graph, this is the top block with bold letters. Then, if additional connections are assumed, we have the contribution of the additional connections on the two-colorable graph to make a three-colorable graph. Finally, the parts that are non-zero but still not indicated in bold represent the connection of the green and the blue qudits with the red ones. If this connection is not maintained, then we would have ended up with two disconnected diagrams, which is not the case for us.

A closing note is that the total number of red qudits is denoted by  $n_R$ , the total number of blue qudits is represented with  $n_B$ , the total number of green qudits is expressed as  $n_G$ , the total number of blue qudits belonging to the set  $B_u$  is symbolized as  $n_{B_u}$  and the total number of blue qudits belonging to the set  $B_c \setminus G$  is indicated as  $n_{B_c \setminus G}$ . Finally, yet importantly, it is assumed without loss of generality that  $n_R \leq n_B + n_G$  and  $n_G \leq n_{B_c \setminus G}$ . At this point, the following proposition can be presented:

**Proposition 3.** *Let us assume a three-colorable graph state described by the adjacency matrix (35), defined as in equation (34), satisfying the set conditions described in the step-by-step construction at the beginning of this section and without loss of generality  $n_R \leq n_{B_u}$ , and  $n_G \leq n_{B_c \setminus G}$ . Then, any such graph state satisfies the following equation:*

$$H^{\dagger \otimes B_c \setminus G} H^{\dagger \otimes B_u} |\psi_{3\text{-color}}\rangle = \sum_{\vec{u}=0}^{d-1} |\vec{u}\mathcal{G}_{B_u R}\rangle \Delta \sum_{\vec{g}=0}^{d-1} |\vec{g}\mathcal{G}_{B_c \setminus G}\rangle, \quad (36)$$

where  $\vec{u} = (u_1, u_2, \dots, u_{n_R})$ ,  $\vec{g} = (g_1, \dots, g_{n_G})$  both row vectors,  $\mathcal{G}_{B_u R} = [\mathbb{I}_{n_R} \mid A_{B_u R}^T]$ ,  $\mathcal{G}_{B_c \setminus G} = [\mathbb{I}_{n_R} \mid A_{GB_c \setminus G}^T]$ ,  $f_{k \in B_c} = \sum_{r \in R} \Gamma_{rk} u_r$ , and the operator  $\Delta$  is defined as following:

$$\Delta = \left( \bigotimes_{i=1}^{n_G} Z_{g_i}^{f_{g_i}} \right) \left( \bigotimes_{j=1}^{n_{B_c \setminus G}} X_{b_j}^{f_{b_j}} \right). \quad (37)$$

The proof of proposition 3 is given in the appendix C. At this juncture, an implication of this proposition must be underlined. Firstly, proposition 3 can be extended to not only the assumed set-up of the three colorable graph states which is depicted in figure 4, where we have only one set of  $B_c$  qudits. It is possible to have  $s$  different numbers of  $B_c$ -like setups that need to

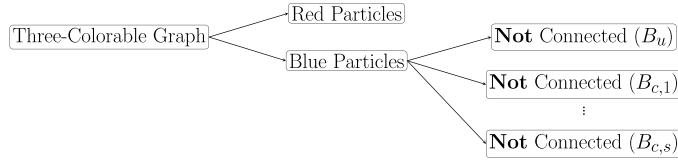


**Figure 5.** A schematic description of the creation of the most general three-colorable graph state studied in this work. In this case we have multiple  $B_c$ -like setups ranging from  $B_{c,1}$  till  $B_{c,s}$ .

obey the same rules. To make it evident, this idea is depicted in figure 5. The extension of the proposition to an arbitrary number of  $s$  different  $B_c$ -like sets is trivial:

$$\bigotimes_{k=1}^s H^{\dagger \otimes B_{c,k} \setminus G_k} H^{\dagger \otimes B_u} |\psi_{3\text{-color}}\rangle = \sum_{\vec{u}=0}^{d-1} |\vec{u}\mathcal{G}_{B_u R}\rangle \bigotimes_{k=1}^s \Delta_k \sum_{\vec{g}^k=0}^{d-1} |\vec{g}^k \mathcal{G}_{B_{c,k} \setminus G_k}\rangle, \quad (38)$$

where each term that got a  $k$  subscript in the equation (38) is trivially extended for any subset  $B_{c,k}$  where  $k = 1, \dots, s$  taking into account the definitions given in the equations (36) and (37).

At this point, the significance of the proposition 3 will be discussed. To begin with, similarly to the case of two-colorable graph states we are equipped with a step-by-step methodology to write the closed-form expression of the discussed three-colorable graph states. Let us present the aforementioned guide of how to use the formula:

- Step 1: Identify the set every node belongs to, namely one should consider 4 sets:  $G, R, B_u, B_c \setminus G$  and ensure that the conditions  $n_R \leq n_{B_u}$  and  $n_G \leq n_{B_c \setminus G}$  are satisfied.
- Step 2: Assign indices on the qudits belonging to the  $R$  and  $G$  sets. Using these indices, find the indices for the blue qudits belonging in the  $B_u$  and the  $B_c \setminus G$ , by adding the indices of their neighbors, precisely like it was done for the 2 colorable cases.
- Step 3: To find the  $\Delta$  operator one has to apply the  $Z$  operations to the green qudits of the  $B_c$  graph and the  $X$  operations to the blue qudits. Then the definition of the function  $f_{k \in B_c} = \sum_{r \in R} \Gamma_{rk} u_r$  must be recalled.
- Step 4: The function  $f_{k \in B_c} = \sum_{r \in R} \Gamma_{rk} u_r$  represents the coupling of the red qudits with the green and blue qudits belonging to the  $B_c$  graph. For this reason, to find the functions  $f_k$  for each qudit in  $B_c$ , one has to find every red qudit that are connected and for each case multiply the index assigned for a red qudit in step 2 and multiply it with the weight between these two vertices. Then, for each qudit belonging to the  $B_c$  set one has to add these coefficients to determine each one of the  $f_{k \in B_c}$ .
- Step 5: Thanks to steps 3 and 4, the  $\Delta$  operator is obtained. Therefore, the final step is to get the result from step 2 for the qudits belonging in the  $B_u$  and  $R$  sets. Then, place the  $\Delta$  operator found in step 4 and finally write the second result of step 2 which is the two-colorable closed-form expression for the  $B_c$  subgraph and the formula of the desired state is found.

A general idea of how proposition 3 works is depicted in figure 6. To make the implementation of the above steps transparent, let us present the application of proposition 3 for two representative examples.

**Example 1.** As the first example, assume the graph state corresponding to the graph given in figure 7. The first step is to ensure the conditions  $n_R \leq n_{B_u}$  and  $n_G \leq n_{B_c \setminus G}$ , which are obeyed

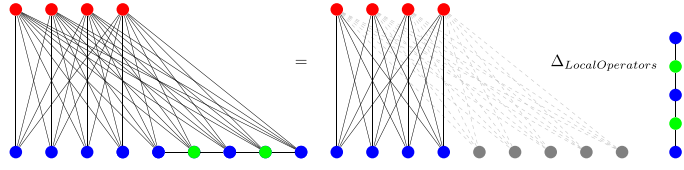


**Figure 6.** An example schematic representation of closed-form expression given in proposition 3. On the left-hand side, the three-colorable graph is shown. On the right-hand side, the two colorable subgraphs are presented. Between them  $\Delta_{LocalOperators}$  is applied. This figure illustrates the process of obtaining the family of states satisfying the required conditions to apply the closed-form expression. In this example on the right-hand side, we have a completely bipartite graph (left of the  $\Delta$ ) and a 1D cluster state (right of  $\Delta$ ). However, this idea extends to any state that satisfies the corresponding conditions.

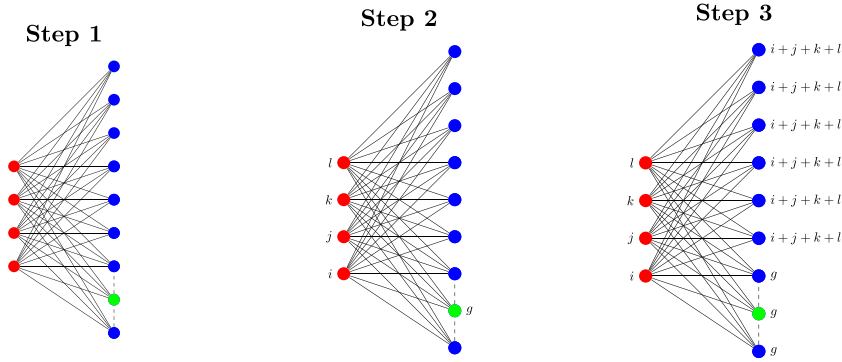


**Figure 7.** Example 1: Presentation of the first three steps of the algorithm to obtain the closed-form expression (42) using proposition 3.

since  $n_R = 4$ ,  $n_{B_u} = 6$ ,  $n_{B_c \setminus G} = 2$  and  $n_G = 1$ . Step 2 requires assigning indices to the green and the red qudits. Step 3 demands to find the indices for the blue qudits, which is simply the addition of the indices found in step 2 of the neighboring indices. This means, that for the connections involving the qudits belonging to the  $R$  and the  $B_u$  set we have:

$$\sum_{i,j,k,l=0}^{d-1} |i\rangle|j\rangle|k\rangle|l\rangle|i+j+k+l\rangle|i+j+k+l\rangle|i+j+k+l\rangle |i+j+k+l\rangle|i+j+k+l\rangle|i+j+k+l\rangle. \tag{39}$$

Similarly, we have the term for the qudits belonging to the  $G$  and the  $B_c \setminus G$  set:

$$\sum_{g=0}^{d-1} |g\rangle|g\rangle|g\rangle. \tag{40}$$

Step 3 requires to construct the  $\Delta$  operator. For this, we know that on the blue qudits of the  $B_c$  graph,  $X$  gates must be applied, while for the green qudit a  $Z$  gate. Step 4 requires determining the function  $f_{k \in B_c}$ , which here is easy since we have assumed that we have weights equal to 1:

$$f_{k \in B_c} = 1 \times i + 1 \times j + 1 \times k + 1 \times l, \tag{41}$$

where the multiplication by one is used to make explicit how the corresponding weight must be used. Bearing the above procedure in mind and combining every step, the final state can be written as:

$$\begin{aligned}
 |\psi_{\text{example-1}}\rangle &= \sum_{i,j,k,l=0}^{d-1} |i\rangle|j\rangle|k\rangle|l\rangle|i+j+k+l\rangle|i+j+k+l\rangle \\
 &\quad |i+j+k+l\rangle|i+j+k+l\rangle|i+j+k+l\rangle|i+j+k+l\rangle \\
 &\quad \left( X_{x_1}^{i+j+k+l} \otimes Z_{x_2}^{i+j+k+l} \otimes X_{x_3}^{i+j+k+l} \right) \sum_{g=0}^{d-1} |g\rangle_{x_1} |g\rangle_{x_2} |g\rangle_{x_3}. \tag{42}
 \end{aligned}$$

It has to be underlined, that in equation (42), the indices  $x_1$  and  $x_3$  represent the blue qudits of the  $B_c$  graph and  $x_2$  the green qudit. In fact, this example has a dual goal. The first was to demonstrate the detailed way to apply the closed-form formula presented in proposition 3. The second one is that if the  $B_c$  graph is a one-dimensional cluster state, the closed-form expression becomes rather interesting. As we explain in the appendix D, in those cases, if  $B_c$  has 2 qudits, then the Bell basis is obtained. When we have 3 qudits the GHZ basis is obtained.

**Example 2.** Let us proceed with the presentation of the second example presented in figure 8. Here in this example, we have two different  $B_c$  sets. This does not have any impact on the application of the step-by-step procedure of the algorithm. In this case, the condition  $n_R \leq n_{B_u}$ ,  $n_{G,1} \leq n_{B_c \setminus G,1}$ , and  $n_{G,2} \leq n_{B_c \setminus G,2}$ , which they do since  $n_R = 4$ ,  $n_{B_u} = 5$ ,  $n_{B_c \setminus G,1} = 1$ ,  $n_{G,1} = 1$ ,  $n_{B_c \setminus G,2} = 1$  and  $n_{G,2} = 1$ . The second step is to assign the indices to the red and the green qudits. Here, we did so for the red qudits, but we have assigned the indices to the blue qudits to make it crystal clear that if  $n_{G,s} = n_{B_c \setminus G,s}$  for whatever  $s$ , then it is irrelevant where the indices will be assigned. In any case, one has to apply them to the same group of colors. Step 3 is straightforward and presented in figure 8. So, we have obtained the summations we intended to. For the connection between the  $R$  and  $B_u$  qudits we have:

$$\begin{aligned}
 &\sum_{i,j,k,l=0}^{d-1} |i\rangle|j\rangle|k\rangle|l\rangle|i+j+k+l\rangle|i+j+k+l\rangle|i+j+k+l\rangle \\
 &\quad |i+j+k+l\rangle|i+j+k+l\rangle, \tag{43}
 \end{aligned}$$

while for the  $B_{c,1}$  and  $B_{c,2}$  we have:

$$\sum_{b_s=0}^{d-1} |b_s\rangle|b_s\rangle, \quad \text{where } s = 1, 2. \tag{44}$$

Step 3 requires to construct the  $\Delta$  operator. For this, we know that on the blue qudits of each  $B_c$  graph,  $X$  gate must be applied, while for the green qudits  $Z$  gate. Step 4 requires determining the function  $f_{k \in B_c}$ , for both  $B_c$  sets assumed in this, which here is easy since we have assumed that we have weights equal to 1:

$$f_{k \in B_{c,s}} = i+j+k+l, \quad \text{where } s = 1, 2. \tag{45}$$

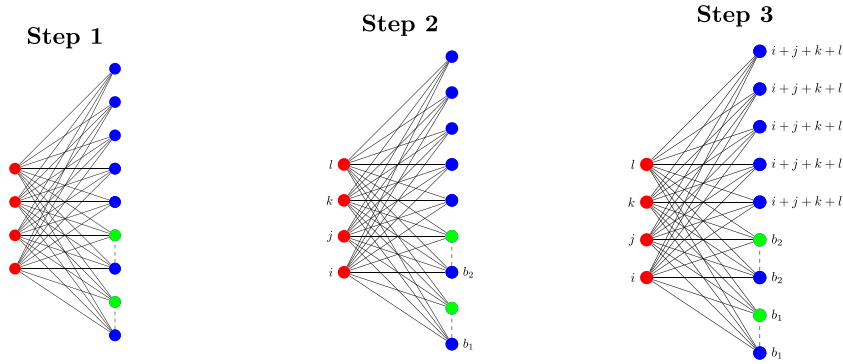


**Figure 8.** Example 2: Presentation of the first three steps of the algorithm to obtain the three-colorable closed-form expression (46) using proposition 3.

Therefore, combining the above results for the graph states depicted in figure 8, the final form is obtained:

$$\begin{aligned}
 |\psi_{\text{example-2}}\rangle &= \sum_{i,j,k,l=0}^{d-1} |i\rangle|j\rangle|k\rangle|l\rangle|i+j+k+l\rangle|i+j+k+l\rangle|i+j+k+l\rangle \\
 &\quad \times |i+j+k+l\rangle|i+j+k+l\rangle \left( X^{i+j+k+l} \otimes Z^{i+j+k+l} \sum_{b_1=0}^{d-1} |b_1\rangle|b_1\rangle \right) \\
 &\quad \otimes \left( X^{i+j+k+l} \otimes Z^{i+j+k+l} \sum_{b_2=0}^{d-1} |b_2\rangle|b_2\rangle \right). \tag{46}
 \end{aligned}$$

The described three-colorable graph state with adjacency matrix, given by equation (35), is, according to the proven proposition 3, on the form of a QOA, therefore every scenario, in which the QOAs are utilized, becomes automatically an interesting area for the assumed family of three-colorable graph states. To be more precise, we refer the reader to equation (38) of the [19]. In this work, it is explained that we can multiply the so-called quantum columns of a QOA. This idea is also apparent in the equation (38) of this work. In section 4, we have explained that every three-colorable graph state is a QOA. In this section, bearing in mind the equation (38) we conclude the same result. In fact, with this methodology, we are presenting a general way to construct QOAs, since we just have to assume several  $B_c$ -like graphs that either have 2 or 3 qudits. In reality, we suspect that we can construct states that are QOAs by concatenating Bell, GHZ, and other AME states of a lower number of qudits in the quantum part of the QOA, but this is a matter of future research. Graphically, this means one can use multiple  $B_c$ -like graphs in the original two-colorable one. The second reason why this setup is important is connected with the construction of  $k$ -uniform states. For this, not only the discussion in this paragraph must be considered, but also the results presented in [28], which will be presented in section 6.3.

A final remark is about the initial condition imposed on the number of  $n_R$  and  $n_{B_u}$  qudits, which must satisfy  $n_R \leq n_{B_u}$ . For this, we have to recall the fact that we can always make an arbitrary graph two-colorable if an adequate number of odd-numbered circles are removed from a non-two-colorable graph. In this case, one has to recall the equation (33) and the fact that  $K$  is the number of vertices removed. What we carried out in practice was the reverse process,

where we started with a two-colorable graph and we started added new edges. The physical implication of the demand that the bound  $n_R \leq n_{B_n}$  is not violated is that, in case it is, then the entanglement properties of the new three-colorable graph state have changed radically, and the correlation with the entanglement properties of the initial two-colorable case is no longer apparent. This result is completely consistent with the fact that the entanglement properties of a state can change only with joint operators. Last but not least, recalling that almost all two-colorable graph states have maximal Schmidt measure [15] for the qubit case, it is rational to examine if it is possible to transform the three-colorable graph state we examined to a two-colorable state. This question will be addressed in the next section.

## 6. Local transformations between two- and three-colorable graph states

### 6.1. Short overview on local transformations

Entanglement characterization is crucial in the study of graph states, making the examination of equivalence classes a natural problem. Moreover, graph states frequently arise in quantum networks, where each vertex represents a spatially separated qudit or laboratory, preventing joint operations [41]. Consequently, quantum operations  $\mathcal{E}$  must be considered as a subclass of completely positive maps (CP maps) that remain separable under the finest partitioning. We are interested in the transformation from state  $|\psi_1\rangle$  to  $|\psi_2\rangle$  with a non-zero probability, if a CP map  $\mathcal{E}$  is adopted. Characterizing the complete class of every transformation  $\mathcal{E}$  that belongs to the local operations and classical communications (LOCCs) is broad and generally challenging. Usually, it is assumed that:

$$\mathcal{E}(\rho) = \bigotimes_{j=1}^N \mathcal{E}_j \rho \bigotimes_{j=1}^N \mathcal{E}_j^\dagger, \quad (47)$$

which means that:  $|\psi_2\rangle = \bigotimes_{j=1}^N \mathcal{E}_j |\psi_1\rangle$ . At this point, let us present three dissimilar classes of local operations [8]. The first one is the invertible stochastic local operations assisted by SLOCC [42], which means that the operation performed in each qudit is of the form  $\mathcal{E}_i \in \text{SL}(d, \mathbb{C})$ . The probability of achieving an SLOCC transformation is typically less than one. Then, the LU equivalence must be taken into account, which means that each operation on every qudit is  $\mathcal{E}_i \in U(d)$ . Finally, the LC are operations on each qudit such that  $\mathcal{E}_i \in \mathcal{C}_1$ , which means they are one of the Clifford unitaries [32]. The last two have the probability of being achieved, if they exist, equal to unity. The generalized Pauli group is generated as follows [32]:

$$\mathcal{P} = \{ \omega^a X^b Z^c \}, \quad \text{with } a, b, c \in \mathbb{F}_d. \quad (48)$$

The  $n$ -body Pauli group  $\mathcal{P}_n$  is defined as the tensor product of  $\mathcal{P}$ . Then, the Clifford group for  $n$  qudits  $\mathcal{C}_n$  can be presented, which is the normalizer of the  $\mathcal{P}_n$ .

### 6.2. Local complementation, LC equivalence, and two-colorable closed-form expression

It is noteworthy that for qubits, there is a simple graphical rule to determine and examine if two graph states are LC equivalent [26] and is called local complementation [25]. The rule is rather simple: one has to choose a vertex, let us assume we call it  $A$ . Then, the neighborhood  $N_A$  of  $A$  must be checked. If two vertices are connected, the edges are deleted, if they are not,

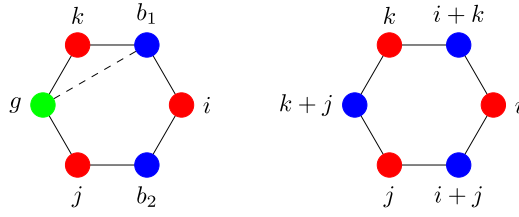


**Figure 9.** An example usage of the Local Complementation to transform a three-colorable graph to a two-colorable graph. On the left, the initial three-colorable graph is given. On the right, the implementation of the method for the closed-form expression is performed.

a connection is established. Additionally, it was shown in [9] that the aforementioned rule is as follows:

$$LC_A = \sqrt{-iX_A} \bigotimes_{b \in N_A} \sqrt{iZ_b}. \tag{49}$$

The idea of a graphical rule to determine LC equivalency has been extended to qudits [32], and the corresponding local transformations are found in [43, 44]. It must be noted that, if two graph states are not LC equivalent, this does not imply that they are also not LU equivalent if the number of qudits is above 8, as it was shown in [45]. In [46], an approach to constructing examples for this case is presented. Finally, one has to bear in mind that the application of LC operations on a graph state does not necessarily lead to a graph state directly, but in general, it should be a stabilizer state [41]. But since stabilizer states can be realized as graph states, as it was shown in [13], every stabilizer state is LC equivalent to some graph state. A final remark is that, even if an efficient algorithm for graphs has been developed [25], as well as the algorithm for the determination of two stabilizer states are LC equivalent, the endeavor of increasing the number of qudits and finding the LC orbit for a large number of qudits turns out to be a challenging goal [47].

In any case, and especially for a small number of qudits, it is always a good idea to find whether a three-colorable graph can be transformed into a two-colorable one by local complementation and then apply the formula found in proposition 1. An example, in this case, is given by figure 9, where local complementation on the qudit indicates that  $k$  eliminates the connection between the qudits  $b_1$  and  $g$ , transforming it into a two-colorable graph state, where the closed-form formula is known.

### 6.3. Association of the presented approach with $k$ -uniform states

The goal of this subsection is to indicate that the three-colorable graph states, assumed in section 5, with the adjacency matrix given by equation (35), arise naturally in the case of the  $k$ -uniform states. In a few words,  $k$ -uniform states are highly entangled pure states, and their property is that all of their  $k$ -qudit reduced density matrices are maximally mixed [17, 19, 28, 48–50]. The way to construct the  $k$ -uniform graph states, presented in [28], fits exactly into the approach of proposition 3. To elaborate on that, it is stated that one has to assume graph states with adjacency matrix given by the following matrix:

$$\Gamma_{k\text{-uniform}} = \left( \begin{array}{c|c} 0 & A \\ \hline A^T & B \end{array} \right). \tag{50}$$

The only requirement is that the matrix  $A$ , as well as each one of its submatrices, are non-singular while the block matrix  $B$  is not limited by anything. It is clear that for  $B = 0$ , a two-colorable graph state is obtained and in proposition 1, the closed-form expression has been given. Additionally, if it is assumed that the matrix  $B$  has the following structure:

$$B = \left( \begin{array}{c|c} 0 & B_1 \\ \hline B_1^T & 0 \end{array} \right), \quad (51)$$

where  $B_1$  and each one of its sub-matrices is non-singular, the so-called hierarchical graph states are created. In this case, the graph state assumed, is simply a special case of the three-colorable graph state described by the adjacency matrix (35). In [28], two important results regarding the SLOCC equivalence are described. In their work, it is interpreted under the scope of  $k$ -uniform states, but as we explained, the colorability understanding is essentially the same. In both cases, the conditions regarding the  $A$  block of the matrix (50) must hold.

They showed that the  $k$ -uniform state with adjacency matrix given by (50) and  $B = 0$ , and the state, given by the same adjacency matrix, and the block  $B$  given by matrix (51), do not belong in the same SLOCC class. In our perspective, this means that we need to consider a general two-colorable graph state described by the matrix (9) and to assume that every submatrix of  $A_{RB}$  is nonsingular. The second stage is to assume we have the three colorable graphs using our approach described by the matrix (35) and just impose that every submatrix of  $G_{B_c \setminus G}$  is non-singular. Then, these two states do not belong to the same SLOCC class.

The second example is to assume a two-colorable graph state, described by the adjacency matrix (9), and impose the conditions to have an AME state. Then, the second graph state is the same as the first one, but the  $B_c$  graph has only two qudits. Then, if the total number of qudits is odd, these two states are not SLOCC equivalent. These two examples showcase that, indeed, in some cases, it is not possible to transform the theorized 3 colorable graph states described by the adjacency matrix (35) to their corresponding two-colorable graph state with the adjacency matrix given by (9).

## 7. $\chi$ -colorable graph states

Generalizing the formalism developed so far, we extend our analysis to graph states with arbitrary colorability  $\chi$ . This requires considering graphs with a chromatic number  $\chi$ , where the vertex set is partitioned into  $\chi$  disjoint color classes. Instead of assigning specific names to the colors, we denote them as color 1, color 2, up to color  $\chi$ , forming corresponding sets of vertices labeled as  $c_1, c_2, \dots, c_\chi$ . The cardinality of each set  $c_l$  (where  $l \in \{1, 2, \dots, \chi\}$ ) is denoted as  $n_l$ . Without loss of generality, we impose the ordering  $n_1 \leq n_2 \leq \dots \leq n_{\chi-1} \leq n_\chi$ . The total number of vertices in the graph is  $n = \sum_{j=1}^{\chi} n_j$ . A  $\chi$ -colorable graph state is defined as:

$$|\psi_{\chi\text{-color}}\rangle = CZ_\chi |+\rangle^{\otimes c_1} |+\rangle^{\otimes c_2} \dots |+\rangle^{\otimes c_\chi} \quad (52)$$

where  $CZ_\chi$  is defined as:

$$CZ_\chi = \prod_{1 \leq i < j \leq \chi} \prod_{p \in c_i, q \in c_j} C_p Z_q^{\Gamma_{p,q}}. \quad (53)$$

The adjacency matrix of a  $\chi$ -colorable graph state is structured as follows:

$$\Gamma_{\chi\text{-color}} = \begin{pmatrix} \overbrace{0}^{c_1} & \overbrace{A_{c_2,c_1}}^{c_2} & \overbrace{\dots}^{\dots} & \overbrace{A_{c_\chi,c_1}}^{c_\chi} \\ A_{c_2,c_1}^T & 0 & \vdots & \vdots \\ \vdots & \vdots & \ddots & \vdots \\ A_{c_\chi,c_1}^T & 0 & A_{c_\chi,c_{\chi-1}}^T & \mathbf{0} \end{pmatrix}. \tag{54}$$

For our upcoming analysis, it is also useful to define the following quantity,

$$Z_{\chi-1} = \bigotimes_{i=2}^{\chi-1} \bigotimes_{j=1}^{n_{c_i}} Z_{c_i,j}^{\sum_{k=1}^{i-1} \vec{v}^{c_k} \cdot (\mathbf{A}_{c_i,c_k})_{c_i,j}}, \tag{55}$$

where the object  $(\mathbf{A}_{c_i,c_k})_{c_i,j}$  is the generalization of the vector defined in proposition 2. Namely, this symbolizes the vector created by the extraction of the column of the block matrix  $A_{c_i,c_k}$  that corresponds to the  $j$ th qudit with color  $c_i$ . We proceed with our analysis by defining a set of vectors as follows:

$$\vec{v}^m = \left( v_1^{c_m}, \dots, v_{n_{c_m}}^{c_m} \right), \quad \text{where, } m \in \{1, \dots, \chi\}. \tag{56}$$

Let us denote the concatenation of every vector  $\vec{v}^{c_l}$ , with  $l \in \{1, \dots, \chi - 1\}$ , starting from  $\vec{v}^{c_1}$  till  $\vec{v}^{c_{\chi-1}}$  as follows:

$$\vec{V}_\chi = (\vec{v}^{c_1}, \dots, \vec{v}^{c_{\chi-1}}). \tag{57}$$

It will also be useful to note that we are going to denote as  $\mathbb{I}_\chi$  the identity matrix of dimension  $\sum_{j=1}^{\chi-1} n_{c_j}$ . Finally, we define a generator-like matrix  $\mathcal{G}_\chi$ , with dimensions  $\left(\sum_{j=1}^{\chi-1} n_{c_j}\right) \times \left(\sum_{j=1}^\chi n_{c_j}\right)$  as:

$$\mathcal{G}_\chi = \left[ \begin{array}{c|c} \mathbb{I}_\chi & \begin{bmatrix} A_{c_\chi,c_1} \\ \vdots \\ A_{c_\chi,c_{\chi-1}} \end{bmatrix} \end{array} \right]. \tag{58}$$

Bearing the above definitions into mind, we have the following proposition, which is a direct generalization of the results obtained in the previous sections.

**Proposition 4.** *A qudit  $\chi$ -colorable graph state defined in equation (52) with the corresponding adjacency matrix of the graph defined in (54) can be written as:*

$$H^{\dagger \otimes c_\chi} |\psi_{\chi\text{-color}}\rangle = \sum_{\vec{V}_\chi=0}^{d-1} Z_{\chi-1} |\vec{V}_\chi \cdot \mathcal{G}_\chi\rangle, \tag{59}$$

with every element used in this proposition defined from the beginning of this section.

**Proof.** The proposition 4 is remarkably straightforward to prove, if the same steps of the proof for proposition 2 are adopted.  $\square$

It is notable that for  $\chi = 3$ , we are reproducing the closed-form expressions presented in the propositions 2 and 3 respectively. Following the thought process of displaying the implications

of each proposition presented, we start by equipping the reader with the step-by-step guide to write the closed-form expression of a  $\chi$ -colorable graph state.

- Step 1: Identify the color of each vertex, with colors starting from  $c_1$  till  $c_{\chi-1}$  and assign indices to them.
- Step 2: The indices of the vertices with color  $c_\chi$  will be the summation of the neighboring indices with color  $c_l$ , where  $l \in \{1, \dots, \chi - 1\}$  multiplied with the corresponding element of the adjacency matrix given by equation (54).
- Step 3: The exponent of the  $Z$  operator for every vertex with color  $c_2$  will be the multiplication of their indices with the indices of the color  $c_1$  weighted with the corresponding element of the adjacency matrix given by equation (54).
- Step 4: We proceed iteratively with the exponents of the  $Z$  gates for every element with a color  $c_l$  where here  $l \in \{2, \dots, \chi - 1\}$  and we multiply their indices with the indices of every vertex with color  $c_{l-1}$  where  $l \in \{2, \dots, \chi - 1\}$ .
- Step 5: We sum over every element of the concatenated vector  $\vec{V}_\chi$ , which has been defined in equation (57).

Applying the same idea as to why every three-colorable is a QOA, it is straightforward to understand that, given the definitions of  $\vec{V}_\chi$  (56) and  $\mathcal{G}_\chi$  (58), the mathematical object  $\vec{V}_\chi \cdot \mathcal{G}_\chi$  forms an OA. Taking into account that we have to apply  $Z_\chi$  and sum-over, we can understand that a  $\chi$ -colorable graph state can be written as a QOA with the following dimensions:

$$\text{QOA} \left( \sum_{j=1}^{\chi-1} n_{c_j}, \sum_{j=1}^{\chi} n_{c_j}, d, k \right) = \text{QOA} (n - n_\chi, n, d, k), \quad (60)$$

where  $k$  satisfies the following relation [19]:

$$k \text{Tr}_{p_1, \dots, p_{n-k}} (|\psi_{\chi\text{-color}}\rangle\langle\psi_{\chi\text{-color}}|) = \left( \sum_{j=1}^{\chi-1} n_{c_j} \right) \mathbb{I}_k, \quad (61)$$

for every subset of  $n - k$  parties  $\{p_1, \dots, p_{n-k}\}$ .

In this work, we have already described multiple times how to derive strict lower bounds on the Schmidt measure of a graph state and how to connect it with the minimum number of terms needed to write the state in the  $Z$ -eigenbasis. The upper bound on Schmidt measure is given by equation (33). Recalling the result of appendix B, for  $\chi \geq 3$  we arrive at:

$$\max \{ \text{rank} (\Gamma_{S|S^c}) \mid S \subset \{c_1, \dots, c_\chi\}, 0 < |S| < \chi/2 \} \leq E_s (|\psi_{\chi\text{-color}}\rangle). \quad (62)$$

The total number of combinations in this case is  $\sum_{k=1}^{\lfloor \frac{\chi}{2} \rfloor} \binom{\chi}{k}$ . Equipped with these results, we point out some important remarks regarding the lower bounds on the Schmidt measure. It is well known that the graph states with a star-shaped graph ( $\chi = 2$ ) is LC equivalent to the GHZ state [8]. It is also trivial to understand that the completely connected graph with  $n$  vertices has  $\chi = n$ . It is well established that the completely connected graph state is LC equivalent to the GHZ state, which means that it is also LC equivalent to the star-shaped graph. Therefore, these three states must have the same Schmidt measure. This makes the discussion very interesting because it illustrates that the endeavor of finding the stricter lower bound for every  $\chi$ -colorable graph state is a much more complicated task. To do so, a numerical approach is to find every state that is LC equivalent to the state we are interested in. Then find the states that have the smallest  $\chi$  and calculate their Schmidt measure. Since the two states are LC equivalent, they

have the same Schmidt measure. This endeavor is a matter of future research, and we hope that the insights given in this work will assist in this.

## 8. Conclusions and outlook

In this work, we have established a systematic approach for deriving closed-form expressions for two- and three-colorable graph states, providing an efficient and intuitive method to represent these states with minimal terms in the  $Z$ -eigenbasis for some cases. We further investigated a special subclass of three-colorable graph states, revealing their natural connection to  $k$ -uniform states. Extending our approach, we formulated a general approach for constructing and analyzing  $\chi$ -colorable graph states. By leveraging graph state colorability, we demonstrated deep connections between QOAs, LC equivalence classes, and multipartite entanglement structure. Our results show that every two-colorable graph state is LC-equivalent to a state expressible via an OA, while all graph states with  $\chi > 2$  are LC-equivalent to a QOA, establishing a direct link between combinatorial designs and quantum information theory.

Beyond formal classification, our results for the closed form expression provided a systematic approach to reduce the classical computation resources required to study graph states and utilize them. The introduced approach enables a compact representation, with direct applications in quantum networks, quantum error correction, and in general, measurement-based quantum computing. Additionally, our generalization to arbitrary  $\chi$ -colorability opens a pathway to systematically characterizing multipartite entanglement classes in graph-based quantum states.

This work opens multiple research directions. While we extended known lower bounds for two- and three-colorable qudit graph states and extended these results to higher  $\chi$ , an open challenge remains to determine the tightest possible bounds for  $\chi$ -colorable graph states and their implications for entanglement distribution in quantum networks. Another fundamental question is the refinement of QOAs. Given that we provided evidence that every OA corresponds to a two-colorable graph state, while QOAs correspond to higher chromatic number states, a deeper mathematical exploration is needed to tighten the connection between QOAs and multipartite entanglement.

By integrating concepts from graph theory, combinatorial designs, and quantum entanglement theory, our work lays a conceptual and practical foundation for the systematic study of graph states. The link between colorability, OAs, and multipartite entanglement provides a novel perspective for constructing and analyzing highly entangled states. We anticipate that these results will be instrumental in advancing quantum state classification, quantum error correction, and scalable quantum computing architectures.

## Data availability statement

No new data were created or analysed in this study.

## Acknowledgments

We thank Edwin Barnes, Adam Burchardt, Sophia Economou, Mario Flory, Markus Grassl, Otfried Gühne, Barbara Kraus, Jan Sperling, Géza Tóth, and Karol Życzkowski for their valuable discussions and remarks. This work was supported by the Equal Opportunity Program, Grant Line 2: Support for Female Junior Professors and Postdocs through Academic Staff Positions, 14th funding round of Paderborn University.

## Appendix A. Some useful properties

Let us present some useful for our analysis relations. The first one is the commutation of  $H^\dagger CZ|kj\rangle$ , which is given by the following equation:

$$H^\dagger CZ|kj\rangle = CXH^\dagger|kj\rangle, \quad (\text{A.1})$$

and it is proven here. Let us assume a two-body state  $|k,j\rangle$  with  $k,j \in \mathbb{Z}_d$ , where  $d$  is the local dimension,

$$H^\dagger CZ|kj\rangle = \omega^{kj}H^\dagger|kj\rangle = \frac{1}{\sqrt{d}}\omega^{kj}|k\rangle \sum_{l=0}^{d-1} \omega^{-lj}|l\rangle. \quad (\text{A.2})$$

On the other hand, let us apply the following assuming the control is happening always on the first qudit:

$$\begin{aligned} CXH^\dagger|kj\rangle &= \frac{1}{\sqrt{d}}CX|k\rangle \sum_{l=0}^{d-1} \omega^{-lj}|l\rangle = \frac{1}{\sqrt{d}}|k\rangle \sum_{l=0}^{d-1} \omega^{-lj}|l+k\rangle \\ &= \frac{1}{\sqrt{d}}\omega^{kj}|k\rangle \sum_{l=0}^{d-1} \omega^{-(l+k)j}|l+k\rangle = \frac{1}{\sqrt{d}}\omega^{kj}|k\rangle \sum_{l'=0}^{d-1} \omega^{-l'j}|l'\rangle. \end{aligned} \quad (\text{A.3})$$

Therefore, the proof is completed. Another useful property is that the  $X$  operator to the power  $a \in \mathbb{F}_d$  is given by the following equation:

$$X^a = H^\dagger Z^a H. \quad (\text{A.4})$$

The above property is proven here. The application of  $X^a$  yields  $X^a|i\rangle = |i+a\rangle$ . While for the  $H^\dagger Z^a H$  we have:

$$\begin{aligned} H|i\rangle &= \sum_{l=0}^{d-1} \omega^{il}|l\rangle \Rightarrow Z^a H|i\rangle = \sum_{l=0}^{d-1} \omega^{il}\omega^{al}|l\rangle \\ H^\dagger Z^a H|i\rangle &= \sum_{m=0}^{d-1} \sum_{l=0}^{d-1} \omega^{il}\omega^{al}\omega^{-ml}|m\rangle, \end{aligned}$$

which leads to  $H^\dagger Z^a H|i\rangle = |i+a\rangle$  and therefore the proof is completed. Finally, a mathematical fact we are going to use extensively in our analysis is:

$$\frac{1}{N} \sum_l \left( \exp\left(\frac{2\pi i}{N}(k-j)\right) \right)^l = \delta_{k,j}, \quad \text{for } k,j \in \mathbb{Z}, \quad (\text{A.5})$$

where  $\delta_{i,j}$  is the Kronecker delta.

## Appendix B. Bounds on Schmidt measure for qudits

Consider a bipartition  $(A, B)$  of a graph  $G = (V, E)$ . Let  $G_{AB}$  represent the subgraph of  $G$  that is imposed by the edges between  $A$  and  $B$ .  $\Gamma_{AB}$  is the  $|A| \times |B|$  diagonal submatrix of  $\Gamma_G$  representing the edges between bipartitions  $A$  and  $B$ :

$$\Gamma_G = \left( \begin{array}{c|c} \Gamma_A & \Gamma_{AB}^T \\ \Gamma_{AB} & \Gamma_B \end{array} \right), \quad \text{and} \quad \Gamma_{G_{AB}} = \left( \begin{array}{c|c} \mathbf{0} & \Gamma_{AB}^T \\ \Gamma_{AB} & \mathbf{0} \end{array} \right). \quad (\text{B.1})$$

Consider a qudit graph state represented by the graph  $G$ . For the measurements of the vertices  $a \in A$  the outcomes are given by  $\{|\bar{z}\rangle = \bigotimes_{a \in A} |\mathbf{z}, \omega^{\bar{z}_a}\rangle\}$ . After the measurement, the graph state  $|G - A\rangle$  is left, and thus the following correction terms based on the measurement outcomes are required:

$$\prod_{a \in A} \prod_{c \in N_a} Z_c^{\dagger \Gamma_{ac} \bar{z}_a} |\bar{z}\rangle \otimes |G - A\rangle = \prod_{a \in A} Z_a^{\dagger \langle \mathbf{e}^a | \Gamma_{G-B} \bar{z} \rangle} \otimes \prod_{b \in B} Z_b^{\dagger \langle \mathbf{e}^b | \Gamma_{AB} \bar{z} \rangle} |G - A\rangle. \quad (\text{B.2})$$

All computations are performed in  $\mathbb{F}_d^A$ , and  $\mathbf{e}_a^b = \delta_{ab}$ . Therefore, the following state vector is obtained:

$$\omega^{\langle \bar{z} | \Gamma_{G-B} \bar{z} \rangle} |\bar{z}\rangle \otimes \prod_{b \in B} Z_b^{\dagger \langle \mathbf{e}^b | \Gamma_{AB} \bar{z} \rangle} |G - A\rangle. \quad (\text{B.3})$$

At this point, we can define the following local unitaries:

$$U(\bar{z}) = \prod_{b \in B} Z_b^{\dagger \langle \mathbf{e}^b | \Gamma_{AB} \bar{z} \rangle}. \quad (\text{B.4})$$

and since  $U(\bar{z}_1)|G - A\rangle$  and  $U(\bar{z}_2)|G - A\rangle$  are orthogonal if and only if  $U(\bar{z}_1 - \bar{z}_2) \neq \mathbb{I}$  the partial trace with respect to any partition  $A$  is:

$$\text{tr}_A(|G\rangle\langle G|) = \frac{1}{d^{|A|}} \sum_{\bar{z} \in \mathbb{F}_d^A} U(\bar{z}) |G\rangle\langle G| U(\bar{z})^\dagger. \quad (\text{B.5})$$

The above equation is crucial because the Schmidt measure of a graph state  $|G\rangle$  with respect to an arbitrary bipartition  $(A, B)$  is given as:

$$E_s(|G\rangle) \geq E_s^{(A,B)}(|G\rangle) = \log_d(\text{rank}(\text{tr}_A(|G\rangle\langle G|))). \quad (\text{B.6})$$

One can easily conclude that:

$$\text{rank}(\text{tr}_A(|G\rangle\langle G|)) = \dim(\text{span}\{U(\bar{z})|G - A\rangle : \bar{z} \in \mathbb{F}_d^A\}). \quad (\text{B.7})$$

Considering for each  $\bar{z}$  the equivalence classes, i.e.  $\{z' \in \mathbb{F}_d^A : U(\bar{z}) = U(z')\}$  for which:

$$\bar{z}' - \bar{z} \in \{\bar{z} \in \mathbb{F}_d^A : U(\bar{z}) = \mathbb{I}\}, \quad (\text{B.8})$$

we have that:

$$\begin{aligned} \log_d(\text{tr}_A(|G\rangle\langle G|)) &= |A| - \log_d \left\{ \bar{z} \in \mathbb{F}_d^A : \langle \mathbf{e}^b | \Gamma_{AB} \bar{z} \rangle =_{\mathbb{F}_d} 0, \forall b \in B \right\} \\ &= |A| - \dim(\ker_{\mathbb{F}_d} \Gamma_{AB}) = \text{rank}_{\mathbb{F}_d}(\Gamma_{AB}), \end{aligned} \quad (\text{B.9})$$

by the rank-nullity theorem.

### Appendix C. Proof of proposition 3

**Proof.** Let us start by applying  $H^{\dagger \otimes B} = H^{\dagger \otimes B_c \cup B_u}$ :

$$\begin{aligned} H^{\dagger \otimes B_c} H^{\dagger \otimes B_u} |q'_{3\text{-color}}\rangle &= H^{\dagger \otimes B_c} \left( \prod_{b, b' \in B_c} C_b Z_b^{\Gamma_{bb'}} \right) \left( \prod_{b \in B_c, r \in R} C_r Z_b^{\Gamma_{br}} \right) \\ &\quad \times H^{\dagger \otimes B_u} \left( \prod_{b \in B_u, r \in R} C_r Z_b^{\Gamma_{br}} \right) |+\rangle^{\otimes R} |+\rangle^{\otimes B_u} |+\rangle^{\otimes B_c}. \end{aligned} \quad (\text{C.1})$$

It is clear that if  $n_R \leq n_{B_u}$  and  $\vec{u} = (u_1, u_2, \dots, u_{n_R})$  a row vector :

$$H^{\dagger \otimes B_u} \left( \prod_{b \in B_u, r \in R} C_b Z_r^{\Gamma_{br}} \right) |+\rangle^{\otimes R} |+\rangle^{\otimes B_u} = \sum_{\vec{u}=0} |\vec{u}\rangle \otimes_{b \in B_u} \left| \sum_{r \in R} \Gamma_{rb} u_r \right\rangle. \quad (\text{C.2})$$

Therefore, it is possible to obtain the following:

$$\begin{aligned} H^{\dagger \otimes B_c} H^{\dagger \otimes B_u} |\psi_{3\text{-color}}\rangle &= \sum_{\vec{u}=0} H^{\dagger \otimes B_c} \left( \prod_{b, b' \in B_c} C_b Z_{b'}^{\Gamma_{bb'}} \right) \left( \prod_{b \in B_c, r \in R} C_b Z_r^{\Gamma_{br}} \right) \\ &\quad |\vec{u}\rangle \otimes_{b \in B_u} \left| \sum_{r \in R} \Gamma_{rb} u_r \right\rangle H^{\otimes B_c} |0\rangle^{\otimes B_c} \\ &= \sum_{\vec{u}=0} H^{\dagger \otimes B_c} \left( \prod_{b, b' \in B_c} C_b Z_{b'}^{\Gamma_{bb'}} \right) \left( \prod_{b \in B_c, r \in R} C_r Z_b^{\Gamma_{br}} \right) \\ &\quad |\vec{u} \mathcal{G}_{B_u R}\rangle H^{\otimes B_c} |0\rangle^{\otimes B_c}, \end{aligned} \quad (\text{C.3})$$

where  $\mathcal{G}_{B_u R} = [\mathbb{I}_{n_R} \mid A_{B_u R}^T]$ . However, this form is not helpful to proceed with our calculation, therefore we are going to expand  $|\vec{u} \mathcal{G}_{B_u R}\rangle$  and use the closed-form expression at the ending point of our proof. The primary goal is to commute  $H^{\dagger \otimes B_c}$  through the two products with the controlled-Z operations. For this reason, the following is performed:

$$H^{\dagger \otimes B_c} \left( \prod_{b, b' \in B_c} C_b Z_{b'}^{\Gamma_{bb'}} \right) = H^{\dagger \otimes B_c} \left( \prod_{b, b' \in B_c} C_b Z_{b'}^{\Gamma_{bb'}} \right) H^{\otimes B_c} H^{\dagger \otimes B_c} = \mathcal{O}_{b, b' \in B_c} H^{\dagger \otimes B_c}. \quad (\text{C.4})$$

For clarification, we have defined an operator named  $\mathcal{O}_{b, b' \in B_c}$  as follows:

$$\mathcal{O}_{b, b' \in B_c} = H^{\dagger \otimes B_c} \left( \prod_{b, b' \in B_c} C_b Z_{b'}^{\Gamma_{bb'}} \right) H^{\otimes B_c}. \quad (\text{C.5})$$

The operator defined in equation (C.5) will help us commutes as following:

$$H^{\dagger \otimes B_c} \left( \prod_{b \in B_c, r \in R} C_b Z_r^{\Gamma_{br}} \right) = \left( \prod_{b \in B_c, r \in R} C_b X_r^{\Gamma_{br}} \right) H^{\dagger \otimes B_c}, \quad (\text{C.6})$$

and thus equation (C.3) can be written as:

$$\begin{aligned} H^{\dagger \otimes B_c} H^{\dagger \otimes B_u} |\psi_{3\text{-color}}\rangle &= \sum_{\vec{u}=0} \mathcal{O}_{b, b' \in B_c} \left( \prod_{r \in R, b \in B_c} C_r X_b^{\Gamma_{rb}} \right) |\vec{u}\rangle \\ &\quad \times \left( \otimes_{b \in B_u} \left| \sum_{r \in R} \Gamma_{rb} u_r \right\rangle \right) |0\rangle^{\otimes B_c}. \end{aligned} \quad (\text{C.7})$$

Finally, using similar steps as the concluding steps in the proof of proposition 1 and recalling that  $n_R \leq n_{B_c}$ :

$$H^{\dagger \otimes B_c} H^{\dagger \otimes B_u} |\psi_{3\text{-color}}\rangle = \sum_{\vec{u}=0} \left( |\vec{u}\rangle \otimes_{b \in B_u} \left| \sum_{r \in R} \Gamma_{rb} u_r \right\rangle \right) \left( \mathcal{O}_{b, b' \in B_c} \otimes_{b \in B_c} \left| \sum_{r \in R} \Gamma_{rb} u_r \right\rangle \right). \quad (\text{C.8})$$

Therefore, one writes the following:

$$H^{\dagger \otimes B_c} H^{\dagger \otimes B_u} |\psi_{3\text{-color}}\rangle = \sum_{\vec{u}=0}^{d-1} |\vec{u}\mathcal{G}_{B_u R}\rangle \left( \mathcal{O}_{b,b' \in B_c} \bigotimes_{b \in B_c} \left| \sum_{r \in R} \Gamma_{rb} u_r \right\rangle \right). \quad (\text{C.9})$$

The connections of the blue qudits imposed in the setup are apparent in the above equation, as well and the fact that the qudits belonging to the  $B_c$  set are still connected with the red qudits is obvious from the coupling in the  $\left| \sum_{r \in R} \Gamma_{rb} u_r \right\rangle$ . Hence, we are going to define the parameter  $f_k$  as follows:

$$f_k = \sum_{r \in R} \Gamma_{rk} u_r. \quad (\text{C.10})$$

This parameter describes the connections of a specific qudit named  $k$  with every red qudit. By construction, the qudits belonging to the  $B_c$  are assumed to be a two-colorable subgraph, and thus the total graph is a three-colorable one. This means that the  $B_c$  graph has qudits that maintain their blue color. These qudits belong to a set which we are going to denote as  $B_c \setminus G$  and this is a set with elements  $B_c \setminus G = \{b'_1, \dots, b'_{n_{B_c \setminus G}}\}$ . Therefore, the total number of qudits belonging to the  $B_c$  graph that maintain their blue color is  $n_{B_c \setminus G}$ . Following the same structure, the  $B_c$  graph has some qudits that became green. Their total number is  $n_G$ , they belong to the set  $G$  and this set has elements denoted as  $G = \{g_1, \dots, g_{n_G}\}$ . With these points in mind, we have that:

$$\bigotimes_{b \in B_c} \left| \sum_{r \in R} \Gamma_{rb} u_r \right\rangle = \bigotimes_{k \in B_c} |f_k\rangle = \bigotimes_{g \in G} |f_g\rangle \bigotimes_{b \in B_c \setminus G} |f_b\rangle. \quad (\text{C.11})$$

Bringing us back to the equation (C.9) we have to calculate the following:

$$\mathcal{O}_{b,b' \in B_c} \bigotimes_{b \in B_c} \left| \sum_{r \in R} \Gamma_{rb} u_r \right\rangle, \quad (\text{C.12})$$

and we will do it in stages. Until this point the cardinality of  $R$ ,  $G$ ,  $B_u$ ,  $B_c$ , and  $B_c \setminus G$  was denoted as  $n_R$ ,  $n_G$ ,  $n_{B_u}$ ,  $n_{B_c}$ , and  $n_{B_c \setminus G}$  respectively. From this point in the equations of our proof we are going to denote it as  $|R|$ ,  $|G|$ ,  $|B_u|$ ,  $|B_c|$ , and  $|B_c \setminus G|$ . Let us start the calculation by applying the Hadamard gates:

$$H^{\otimes G} H^{\otimes B_c \setminus G} \bigotimes_{g \in G} |f_g\rangle \bigotimes_{b \in B_c \setminus G} |f_b\rangle = \sum_{l_{g_1}, \dots, l_{g_{|G|}}=0}^{|G|} \sum_{l_{b'_1}, \dots, l_{b'_{|B_c \setminus G|}}=0}^{|B_c \setminus G|} \omega^{\sum_{i=1}^{|G|} l_{g_i} f_{g_i} + \sum_{i=1}^{|B_c \setminus G|} l_{b'_i} f_{b'_i}} |l_{g_1}, \dots, l_{g_{|G|}}\rangle |l_{b'_1}, \dots, l_{b'_{|B_c \setminus G|}}\rangle. \quad (\text{C.13})$$

To introduce a short-hand notation, instead of  $\sum_{l_{g_1}, \dots, l_{g_{|G|}}=0}^{|G|}$  we are going to write  $\sum_{l_g}$ . Similarly instead  $\sum_{l_{b'_1}, \dots, l_{b'_{|B_c \setminus G|}}=0}^{|B_c \setminus G|}$  we will write  $\sum_{l_b}$ . After these clarifications, we have to proceed with the application of the corresponding controlled-Z operations. For this, we have to keep in mind the following:

$$\prod_{b,b' \in B_c} CZ^{\Gamma_{bb'}} = \prod_{g \in G, b \in B_c \setminus G} CZ^{\Gamma_{gb}}. \quad (\text{C.14})$$

Therefore we have that:

$$\begin{aligned} & \left( \prod_{g \in G, b \in B_c \setminus G} CZ^{\Gamma_{gb}} \right) H^{\otimes G} H^{\otimes B_c \setminus G} \bigotimes_{g \in G} |f_g\rangle \bigotimes_{b \in B_c \setminus G} |f_b\rangle \\ &= \sum_{l_g} \sum_{l_b} \Omega \left( \sum_{i=1}^{|G|} l_g f_{g_i} + \sum_{i=1}^{|B_c \setminus G|} l_{b'_i} f_{b'_i} + \sum_{i=1}^{|G|} \sum_{j=1}^{|B_c \setminus G|} l_{g_i} l_{b_j} \Gamma_{g_i b'_j} \right) \\ & |l_{g_1}, \dots, l_{g_{|G|}}\rangle |l_{b'_1}, \dots, l_{b'_{|B_c \setminus G|}}\rangle, \end{aligned} \tag{C.15}$$

where  $\Omega(x) = \omega^x$  for  $x \in \mathbb{R}$ . At this stage, the fact that the subgraph  $B_c$  is two-colorable and that without loss of generality it is assumed that  $|G| \leq |B_c \setminus G|$  is crucial. In the same way, as we did for the two colorable cases, instead of applying  $H^{\dagger \otimes B_c \setminus G} H^{\dagger \otimes G}$ , we apply only the  $H^{\dagger \otimes B_c \setminus G}$ . This can be done trivially since  $H^{\otimes G} H^{\dagger \otimes B_c \setminus G} H^{\dagger \otimes G} = H^{\dagger \otimes B_c \setminus G}$ . Therefore we have that:

$$\begin{aligned} & H^{\dagger \otimes B_c \setminus G} \left( \prod_{g \in G, b \in B_c \setminus G} CZ^{\Gamma_{gb}} \right) H^{\otimes G} H^{\otimes B_c \setminus G} \bigotimes_{g \in G} |f_g\rangle \bigotimes_{b \in B_c \setminus G} |f_b\rangle \\ &= \sum_{l_g} \sum_{l_b} \sum_{m_b} \Omega \left( \sum_{i=1}^{|G|} l_g f_{g_i} + \sum_{i=1}^{|B_c \setminus G|} l_{b'_i} f_{b'_i} + \sum_{i=1}^{|G|} \sum_{j=1}^{|B_c \setminus G|} l_{g_i} l_{b'_j} \Gamma_{g_i b'_j} - \sum_{i=1}^{|B_c \setminus G|} l_{b'_i} m_{b'_i} \right) \\ & |l_{g_1}, \dots, l_{g_{|G|}}\rangle |m_{b'_1}, \dots, m_{b'_{|B_c \setminus G|}}\rangle, \end{aligned}$$

where the summation  $\sum_{m_b}$  denotes the following summation:  $\sum_{m_{b'_1}, \dots, m_{b'_{|B_c \setminus G|}} = 0}$ . Our goal is to use the property of the Kronecker delta that is given in equation (A.5) using as summation the sums of the  $l_b$  indices since they are not a part of the ket in the above equation. For this reason, we have to define the quantity  $p_a$  as:

$$p_a = f_{b'_a} + \sum_{i=1}^{|G|} l_{g_i} \Gamma_{b'_a g_i}, \tag{C.16}$$

which underlines the structure of the theorized graph. Initially, the letter  $a$  in subscript denotes a blue qudit indicated with the index  $a$  following the equation (C.10). Subsequently, the second term in the equation (C.16) represents the additional connections we imposed to form the  $B_c$  graph and therefore represents the connections between the blue qudits belonging to the set  $B_c \setminus G$  and the green qudits which belong to the set  $G$ . Thus, taking into consideration equation (C.16):

$$\begin{aligned} & H^{\dagger \otimes B_c \setminus G} \left( \prod_{g \in G, b \in B_c \setminus G} CZ^{\Gamma_{gb}} \right) H^{\otimes G} H^{\otimes B_c \setminus G} \bigotimes_{g \in G} |f_g\rangle \bigotimes_{b \in B_c \setminus G} |f_b\rangle \\ &= \sum_{l_g} \sum_{m_b} \delta_{p_1, m_1} \dots \delta_{p_{|B_c \setminus G|}, m_{|B_c \setminus G|}} \times \Omega \left( \sum_{i=1}^{|G|} l_g f_{g_i} \right) |l_{g_1}, \dots, l_{g_{|G|}}\rangle |m_{b_1}, \dots, m_{b_{|B_c \setminus G|}}\rangle, \end{aligned} \tag{C.17}$$

and therefore we obtain that:

$$H^{\dagger \otimes B_c \setminus G} \left( \prod_{g \in G, b \in B_c \setminus G} CZ^{\Gamma_{gb}} \right) H^{\otimes G} H^{\otimes B_c \setminus G} \bigotimes_{g \in G} |f_g\rangle \bigotimes_{b \in B_c \setminus G} |f_b\rangle \quad (\text{C.18})$$

$$= \sum_{l_g} \Omega \left( \sum_{i=1}^{|G|} l_{g_i} f_{g_i} \right) |l_{g_1}, \dots, l_{g_{|G|}}\rangle |p_{g_1}, \dots, p_{g_{|G|}}\rangle. \quad (\text{C.19})$$

A careful inspection of the equation (C.18) leads us to write it as:

$$H^{\dagger \otimes B_c \setminus G} \left( \prod_{g \in G, b \in B_c \setminus G} CZ^{\Gamma_{gb}} \right) H^{\otimes G} H^{\otimes B_c \setminus G} \bigotimes_{g \in G} |f_g\rangle \bigotimes_{b \in B_c \setminus G} |f_b\rangle \quad (\text{C.20})$$

$$= \left( \bigotimes_{i=1}^{n_G} Z_{g_i}^{f_{g_i}} \right) \left( \bigotimes_{j=1}^{n_{B_c \setminus G}} X_{b_j}^{f_{b_j}} \right) \sum_{l_g} |l_{g_1}, \dots, l_{g_{n_G}}\rangle \bigotimes_{m=1}^{n_{B_c \setminus G}} \left| \sum_{k=1}^{n_G} l_{g_k} \Gamma_{b_m g_k} \right\rangle.$$

It must be underlined that the notation of cardinality of the sets is switched to the one we adopted at the beginning. To introduce a more effective notation in our equations, let us define the operator  $\Delta$ :

$$\Delta = \left( \bigotimes_{i=1}^{n_G} Z_{g_i}^{f_{g_i}} \right) \left( \bigotimes_{j=1}^{n_{B_c \setminus G}} X_{b_j}^{f_{b_j}} \right). \quad (\text{C.21})$$

Likewise the proof for proposition 1, we will define a row vector  $\vec{g} = (g_1, \dots, g_{n_G})$  and a matrix  $\mathcal{G}_{B_c \setminus G} = \left[ \mathbb{I}_{n_R} \mid A_{G B_c \setminus G}^T \right]$ , where  $A_{G B_c \setminus G}$  is the corresponding block of the matrix (35). Therefore, the remaining part in the parenthesis of equation (C.9) is calculated and we arrive at:

$$H^{\dagger \otimes B_c} H^{\dagger \otimes B_u} |\psi_{3\text{-color}}\rangle = \sum_{u_1, \dots, u_{n_R}=0}^{d-1} |\vec{u}_{G B_u R}\rangle \Delta \left( \sum_{g_1, \dots, g_{n_G}=0}^{d-1} |\vec{g}_{B_c \setminus G}\rangle \right), \quad (\text{C.22})$$

which concludes our proof.  $\square$

### Appendix D. One dimensional cluster states and circles as the $B_c$ subgraph

The goal of this subsection is to study  $B_c$  graphs with specific structures, that can lead to interesting cases of three-colorable graphs. Let us start by assuming that the  $B_c$  graph is a one-dimensional cluster state with an arbitrary number of qudits, denoted as  $k$ . To better illustrate it, figure D1 is such an example with  $k=9$  qudits. We are going to derive our closed-form formula stated in the proposition 3, but not starting entirely from the beginning, but rather from the action of the  $\mathcal{O}_{b, b' \in B_c}$  on an arbitrary ket  $|l_1, \dots, l_k\rangle$ . Let us initiate the analysis by implementing the equation (C.5) on this context:

$$\mathcal{O}_{x, x' \in B_c} = \left( \prod_{x=1}^{k-1} H_{x_j}^{\dagger} \right) \left( \prod_{x=1}^{k-1} C_{x_j} Z_{x_{j+1}}^{\Gamma_{x_j x_{j+1}}} \right) \left( \prod_{x=1}^k H_{x_j} \right). \quad (\text{D.1})$$

Therefore the action of the above operator on an arbitrary state  $|i_1, \dots, i_k\rangle$  is:



**Figure D1.** A one-dimensional cluster state with nine vertices as the  $B_c$  subgraph.

$$\begin{aligned} & \left( \prod_{k=1}^{k-1} C_{x_j} Z_{x_{j+1}}^{\Gamma_{x_j x_{j+1}}} \right) \left( \prod_{k=1}^k H_{x_j} \right) |i_1, \dots, i_k\rangle \\ &= \sum_{l_1, \dots, l_k=0}^{d-1} \Omega \left( \sum_{j=1}^k l_j i_j + \sum_{j=1}^{k-1} l_j l_{j+1} \Gamma_{x_j x_{j+1}} \right) |l_1, \dots, l_k\rangle. \end{aligned} \quad (\text{D.2})$$

It is assumed that the chain contains an odd number of terms. The steps for the even-numbered case are the same and thus are omitted. Therefore, the last qudit is denoted as  $x_{2j+1}$ . Bearing in mind that for the  $B_c$  qudits  $n_G \leq n_{B_c \setminus G}$ , the blue qudits are always of the form  $x_{2j+1}$  (odd-numbered  $j$ ), and the green qudits are always of the form  $x_{2j}$  (even numbered  $j$ ). Acknowledging the discussion about the number of  $H^\dagger$  we can apply to decrease the number of terms, only the odd-numbered  $H^\dagger$  will be performed and therefore the following is obtained. This was explained in appendix C. After a few lines of calculations, we have that:

$$\begin{aligned} & \left( \prod_{j=0}^k H_{x_{2j+1}}^\dagger \right) \left( \prod_{j=1}^{k-1} C_{x_j} Z_{x_{j+1}}^{\Gamma_{x_j x_{j+1}}} \right) \left( \prod_{j=1}^k H_{x_j} \right) |i_1, \dots, i_k\rangle \\ &= \sum_{l_1, \dots, l_k=0}^{d-1} \sum_{m_1, \dots, m_{2k+1}=0}^{d-1} \Omega \left( \sum_{j=1}^k l_j i_j - \sum_{j=1}^k m_{2j-1} l_{2j-1} + \sum_{j=1}^{k-1} l_j l_{j+1} \Gamma_{x_j x_{j+1}} \right) \\ & \quad |m_1, l_2, m_3, \dots, m_{2k+1}\rangle. \end{aligned}$$

Taking into account equation (A.5) we arrive at:

$$\begin{aligned} \mathcal{O}_{x, x' \in B_c} |i_1, \dots, i_k\rangle &= \sum_{l_2, \dots, l_{2k}=0}^{d-1} \Omega \left( \sum_{j=1}^{d-1} l_{2j} i_{2j} \right) \\ & \quad |i_1 + l_2 \Gamma_{x_1 x_2}, l_2, i_3 + l_2 \Gamma_{x_3 x_2} + l_4 \Gamma_{x_3 x_4}, \dots\rangle. \end{aligned} \quad (\text{D.3})$$

After some algebraic manipulations, equation (D.3) can be written with respect to the operators  $X$  and  $Z$ :

$$\mathcal{O}_{x, x' \in B_c} |i_1, \dots, i_k\rangle = \bigotimes_{j=0}^k X_{x_{2j+1}}^{i_{2j+1}} \bigotimes_{j=0}^k Z_{x_{2j}}^{i_{2j}} \sum_{l_2, \dots, l_{2k}=0}^{d-1} |l_2 \Gamma_{x_1 x_2}, l_2, \dots, l_{2k} \Gamma_{x_{2k} x_{2k+1}}\rangle. \quad (\text{D.4})$$

Equation (D.4) allows for some intriguing conclusions. If two qudits are assumed to belong in the  $B_c$  subgraph, then the following is obtained:

$$\mathcal{O}_{x_1, x_2 \in B_c} |i\rangle_{x_1} |j\rangle_{x_2} = X_{x_1}^i \otimes Z_{x_2}^j \sum_{l=0}^{d-1} |l\rangle_{x_1} |l\rangle_{x_2}, \quad (\text{D.5})$$

which is the Bell basis. To make it more obvious, let us assume we work with qubits and therefore  $d = 2$ :

$$\mathcal{O}_{x_1, x_2 \in B_c} |i, j\rangle = |i, 0\rangle + (-1)^j |i + 1, 1\rangle. \quad (\text{D.6})$$

This means that the following correspondence is obtained:

$$\begin{aligned} |00\rangle &\rightarrow |00\rangle + |11\rangle = |\Phi^+\rangle \\ |01\rangle &\rightarrow |00\rangle - |11\rangle = |\Phi^-\rangle \\ |10\rangle &\rightarrow |10\rangle + |01\rangle = |\Psi^+\rangle \\ |11\rangle &\rightarrow -|10\rangle + |01\rangle = -|\Psi^-\rangle, \end{aligned} \quad (\text{D.7})$$

where  $\Phi^\pm$  and  $\Psi^\pm$  are the four Bell states for the qubit case. Similarly, for three qudits belonging to the  $B_c$  set, the GHZ state is obtained:

$$\mathcal{O}_{x_1, x_2, x_3 \in B_c} |i_1, i_2, i_3\rangle = X_{x_1}^{i_1} \otimes Z_{x_2}^{i_2} \otimes X_{x_3}^{i_3} \sum_{l=0}^{d-1} |l\rangle_{x_1} |l\rangle_{x_2} |l\rangle_{x_3}. \quad (\text{D.8})$$

It must be noted that for simplicity in the above example, the values of the adjacency matrix elements are assumed to be one. This is the case as well for the upcoming example where the result for 4 qudits is presented:

$$\mathcal{O}_{b, b' \in B_c} |i_1, i_2, i_3, i_4\rangle = X_{b_1}^{i_1} \otimes Z_{b_2}^{i_2} \otimes X_{b_3}^{i_3} \otimes Z_{b_4}^{i_4} \sum_{l_2, l_4=0}^{d-1} |l_2, l_2, l_2 + l_4, l_4\rangle. \quad (\text{D.9})$$

This is a rather interesting result, especially if we realize that we can manipulate the previous equation and arrive at:

$$H_{b_3} H_{b_4}^\dagger \mathcal{O}_{b, b' \in B_c} |i_1, i_2, i_3, i_4\rangle = X_{b_1}^{i_1} \otimes Z_{b_2}^{i_2} \otimes Z_{b_3}^{i_3} \otimes X_{b_b}^{i_4} \sum_{l, m=0}^{d-1} \omega^{lm} |l, l\rangle \otimes |m, m\rangle.$$

This result can be generalized for any number of qudits and implies two facts. The first is that indeed the number of  $H^\dagger$  operations one should apply for the final step of the calculation of the operator defined in general in equation (C.5) remains  $H^{\dagger \otimes B_c \setminus G}$ . The second fact is that it is possible to write part, if not the whole ket, inside the D.4 as a tensor product having combinations of  $|l, l\rangle$  or  $|l, l, l\rangle$ . This is rather important for the discussion of the equivalence using local operators between the state  $|\psi_{2\text{-color}}\rangle$  and the state  $|\psi_{3\text{-color}}\rangle$ .

At this point, it has to be noted that in the given examples, the value of the adjacency matrix is assumed to be one. We recall that every possible value inside the kets belongs to  $\mathbb{F}_d$ , which is also true for every possible value of the adjacency matrix. The multiplication of any element belonging to  $\mathbb{F}_d$  with any other element belonging to the same field maps to an element in  $\mathbb{F}_d$ . This allows us to understand that showing that the Bell or GHZ state is obtained assuming every adjacency matrix to be 1 can be generalized for any combination of values for the adjacency matrices.

Let us proceed with the  $B_c$  qudits creating a circle with an even number of qudits to create a two-colorable subgraph. Equipped with the previously presented results, it is easy to conclude that if the  $B_c$  graph is an even-numbered circle then the action of the operator  $\mathcal{O}_{b, b' \in B_c}$  is given

by the following equation:

$$\mathcal{O}_{b,b' \in B_c} |c_1, \dots, c_{2N}\rangle = \bigotimes_{j=0}^k X_{b_{2j+1}}^{c_{2j+1}} \bigotimes_{j=0}^k Z_{b_{2j}}^{c_{2j}} \sum_{l_2, \dots, l_{2N}=0}^{d-1} |l_2 \Gamma_{b_1 b_2} + l_{2N} \Gamma_{b_1 b_{2N}}, l_2, \dots\rangle.$$

This result is connected with the obtained in the equation (D.4), which is expected, since the only difference between the first and the second setup is that the first and the last qudits are connected in the latter case.

## ORCID iDs

Konstantinos-Rafail Revis  0000-0002-5645-5448

Hrachya Zakaryan  0009-0009-2862-2243

Zahra Raissi  0000-0002-9168-8212

## References

- [1] Horodecki R, Horodecki P, Horodecki M and Horodecki K 2009 Quantum entanglement *Rev. Mod. Phys.* **81** 865–942
- [2] Datta C, Kondra T V, Miller M and Streltsov A 2022 Entanglement catalysis for quantum states and noisy channels *Quantum* **8** 1290
- [3] Scott A J 2004 Multipartite entanglement, quantum-error-correcting codes and entangling power of quantum evolutions *Phys. Rev. A* **69** 052330
- [4] Calderbank A R, Rains E M, Shor P M and Sloane N J A 1998 Quantum error correction via codes over GF(4) *IEEE Trans. Inf. Theory* **44** 1369–87
- [5] Gottesman D 2009 An introduction to quantum error correction and fault-tolerant quantum computation (arXiv:0904.2557)
- [6] Cirac J I, Zoller P, Kimble H J and Mabuchi H 1997 Quantum state transfer and entanglement distribution among distant nodes in a quantum network *Phys. Rev. Lett.* **78** 3221–4
- [7] Hillery M, Bužek V and Berthiaume A 1999 Quantum secret sharing *Phys. Rev. A* **59** 1829–34
- [8] Hein M, Dür W, Eisert J, Raussendorf R, Van den Nest M and Briegel H J 2006 Entanglement in graph states and its applications (arXiv:quant-ph/0602096)
- [9] Hein M, Eisert J and Briegel H J 2004 Multipartite entanglement in graph states *Phys. Rev. A* **69** 062311
- [10] Raussendorf R, Browne D and Briegel H 2002 The one-way quantum computer—a non-network model of quantum computation *J. Mod. Opt.* **49** 1299–306
- [11] Raissi Z, Teixidó A, Gogolin C and Acín A 2020 Constructions of  $k$ -uniform and absolutely maximally entangled states beyond maximum distance codes *Phys. Rev. Res.* **2** 033411
- [12] Raissi Z, Gogolin C, Riera A and Acín A 2018 Optimal quantum error correcting codes from absolutely maximally entangled states *J. Phys. A: Math. Theor.* **51** 075301
- [13] Schlingemann D 2001 Stabilizer codes can be realized as graph codes (arXiv:quant-ph/0111080)
- [14] Cohen G D, Honkala I S, Litsyn S and Lobstein A 1997 Basic Facts *Covering Codes (North-Holland Mathematical Library vol 54)* (Elsevier) p 55
- [15] Severini S 2006 Two-colorable graph states with maximal schmidt measure *Phys. Lett. A* **356** 99–103
- [16] Hedayat A S, Sloane N J A and Stufken J 1999 *Orthogonal Arrays: Theory and Applications* (Springer) (<https://doi.org/10.1007/978-1-4612-1478-6>)
- [17] Goyeneche D and Życzkowski K 2014 Genuinely multipartite entangled states and orthogonal arrays *Phys. Rev. A* **90** 022316
- [18] Seveso L, Goyeneche D and Życzkowski K 2017 All orthogonal arrays from quantum states (arXiv:1709.05916v2)

- [19] Goyeneche D, Raissi Z, Di Martino S and Życzkowski K 2018 Entanglement and quantum combinatorial designs *Phys. Rev. A* **97** 062326
- [20] Zha X-W, Ahmed I, Imran M, Rizvi S M A, Magsi H and Zhang Y 2023 Phase parameters of orthogonal arrays and special maximally multi-qubit entangled states *Mod. Phys. Lett. B* **38** 2450133
- [21] Zang Y, Tian Z, Fei S and Zuo H 2023 Quantum k-uniform states from quantum orthogonal arrays *Int. J. Theor. Phys.* **62** 1–22
- [22] Lin X, Pang S and Wang J 2024 Construction of asymmetric orthogonal arrays with high strength *Stat* **13** e70011
- [23] Rötteler M and Wocjan P 2004 Equivalence of decoupling schemes and orthogonal arrays *IEEE Trans. Inf. Theory* **52** 4171–81
- [24] Burchardt A and Raissi Z 2020 Stochastic local operations with classical communication of absolutely maximally entangled states *Phys. Rev. A* **102** 022413
- [25] Bouchet A 1993 Recognizing locally equivalent graphs *Discrete Math.* **114** 75–86
- [26] Van den Nest M, Dehaene J and De Moor B 2004 Graphical description of the action of local clifford transformations on graph states *Phys. Rev. A* **69** 022316
- [27] Van den Nest M, Dehaene J and De Moor B 2004 Efficient algorithm to recognize the local clifford equivalence of graph states *Phys. Rev. A* **70** 034302
- [28] Raissi Z, Burchardt A and Barnes E 2022 General stabilizer approach for constructing highly entangled graph states *Phys. Rev. A* **106** 062424
- [29] West D B 2001 *Introduction to Graph Theory* 2nd edn (Prentice Hall)
- [30] Diestel R 2005 *Graph Theory (Graduate Texts in Mathematics)* (Springer) (<https://doi.org/10.1007/978-3-662-70107-2>)
- [31] Keet A, Fortescue B, Markham D and Sanders B C 2010 Quantum secret sharing with qudit graph states *Phys. Rev. A* **82** 062315
- [32] Bahramgiri M and Beigi S 2007 Graph states under the action of local clifford group in non-binary case (arXiv:[quant-ph/0610267](https://arxiv.org/abs/quant-ph/0610267))
- [33] Raissi Z, Barnes E and Economou S E 2024 Deterministic generation of qudit photonic graph states from quantum emitters *PRX Quantum* **5** 020346
- [34] Dür W, Aschauer H and Briegel H-J 2003 Multiparticle entanglement purification for graph states *Phys. Rev. Lett.* **91** 107903
- [35] Zander R and Becker C K-U 2024 Benchmarking multipartite entanglement generation with graph states (arXiv:[2402.00766](https://arxiv.org/abs/2402.00766))
- [36] Eisert J and Briegel H J 2001 Schmidt measure as a tool for quantifying multiparticle entanglement *Phys. Rev. A* **64** 022306
- [37] Karp R M 1972 Reducibility Among Combinatorial Problems *Complexity of Computer Computations (The IBM Research Symposia Series)* (Springer) pp 85–103
- [38] Stockmeyer L 1973 Planar 3-colorability is polynomial complete *SIGACT News* **5** 19–25
- [39] Lovasz L 1973 Coverings and colorings of hypergraphs *Proc. 4th Southeastern Conf. on Combinatorics, Graph Theory and Computing* pp 3–12 (available at: <http://www.cs.elte.hu/~lovasz/scans/covercolor.pdf>)
- [40] Seveso L, Goyeneche D and Życzkowski K 2018 Coarse-grained entanglement classification through orthogonal arrays *J. Math. Phys.* **59** 072203
- [41] Vandr e L, de Jong J, Hahn F, Burchardt A, G uhne O and Pappa A 2024 Distinguishing graph states by the properties of their marginals (arXiv:[2406.09956](https://arxiv.org/abs/2406.09956))
- [42] D ur W, Vidal G and Cirac J I 2000 Three qubits can be entangled in two inequivalent ways *Phys. Rev. A* **62** 062314
- [43] Booth R I and Carette T 2022 Complete zx-calculi for the stabiliser fragment in odd prime dimensions *47th International Symposium on Mathematical Foundations of Computer Science (MFCS 2022) (Leibniz International Proceedings in Informatics (LIPIcs) vol 241)* (Schloss Dagstuhl – Leibniz-Zentrum f ur Informatik) pp 24:1–24:15
- [44] Booth R I 2022 Measurement-based quantum computation beyond qubits Sorbonne Universit e tel-03867179
- [45] Ji Z, Chen J, Wei Z and Ying M 2008 The lu-lc conjecture is false (arXiv:[0709.1266](https://arxiv.org/abs/0709.1266))
- [46] Tsimakuridze N and G uhne O 2017 Graph states and local unitary transformations beyond local clifford operations *J. Phys. A: Math. Theor.* **50** 195302

- [47] Adcock J C, Morley-Short S, Dahlberg A and Silverstone J W 2020 Mapping graph state orbits under local complementation *Quantum* **4** 305
- [48] Latorre J I and Sierra G 2015 Holographic codes (arXiv:1502.06618)
- [49] Raissi Z 2020 Modifying method of constructing quantum codes from highly entangled states *IEEE Access* **8** 222439–48
- [50] Pastawski F, Yoshida B, Harlow D and Preskill J 2015 Holographic quantum error-correcting codes: toy models for the bulk/boundary correspondence *J. High Energy Phys.* **JHEP06(2015)149**